NASA Technical Memorandum 78719

Impact Tests on Fibrous Composite Sandwich Structures

Marvin D. Rhodes

OCTOBER 1978

NASA

NASA Technical Memorandum 78719

Impact Tests on Fibrous Composite Sandwich Structures

Marvin D. Rhodes
Langley Research Center
Hampton, Virginia

NASA
National Aeronautics
and Space Administration

Scientific and Technical Information Office

1978

SUMMARY

An experimental investigation examined the effect of low-velocity impact on the strength of laminates fabricated from graphite/epoxy and Kevlar[1] 49/epoxy composite materials. The test laminates were loaded statically either in uniaxial tension or compression when impact occurred to evaluate the effect of loading on the initiation of damage and/or failure. Typical aircraft service conditions such as runway debris encountered during landing were simulated by impacting 1.27-cm-diameter projectiles normal to the plane of the test laminates at velocities between 5.2 and 48.8 m/s.

Results of this investigation indicate that low-velocity impact at energy levels below that necessary to create visible surface damage initiated catastrophic failures in all test laminates loaded in either tension or compression. Reductions in compression strength due to impact were greater for some laminates than reductions in tensile strength. The use of materials such as Kevlar 49 to form graphite hybrids did improve the impact strength of some laminates loaded in compression; however, there was no improvement in the impact strength of hybrids loaded in tension.

INTRODUCTION

Tolerance to low-velocity impact damage should be considered in the evaluation of advanced composite structures designed for aircraft applications. Test results reported in references 1 and 2 show that: (1) low-velocity projectile impacts can initiate structural failures in both tension- and compression-stressed composite laminates; and (2) visual observations are inadequate to identify impact-initiated damage which can significantly degrade structural properties. These test specimens were of a limited number of lamina orientations, stacking sequences, and thicknesses; and, therefore, conclusions of a general nature cannot be drawn from the results.

The purpose of the present paper is to expand the limited data base contained in reference 2 by examining a number of laminates that are representative of the type proposed for secondary aircraft structures. All laminates were tested using conventional four-point beam-bending sandwich specimens with graphite/epoxy and/or Kevlar 49/epoxy face sheets. All laminate specimens were loaded statically either in uniaxial tension or compression when impact occurred. Some specimens failed catastrophically at the instant of impact, some did not. Specimens which did not fail catastrophically, however, had some local damage and were subsequently statically tested to evaluate the effect of local damage on residual strength. The impact projectiles used in this investigation were 1.27-cm-diameter spheres, and impact velocities ranged from 5.2 to 48.8 m/s. These choices simulate typical impact conditions involving runway debris encountered during aircraft operation.

---

[1] Kevlar: Trade name of E. I. duPont de Nemours & Co., Inc.

Identification of commercial products in this report is used to describe adequately the test materials. The identification of these commercial products does not constitute official endorsement, expressed or implied, of such products by the National Aeronautics and Space Administration.

SYMBOLS

P	static load prior to impact
P_{ult}	average ultimate load of undamaged test specimens
ϵ	strain

MATERIALS AND SPECIMENS

Materials

The materials used to fabricate test specimens were high-strength graphite fibers and/or Kevlar 49 fibers in a 450K-cure commercially available epoxy resin. These materials were used in both woven fabrics and unidirectional fiber tapes. Typical properties of these materials are given in table I. All materials were supplied in pre-impregnated form and processed according to the manufacturer's recommendations. These materials were selected because they have received widespread usage and an acceptable data base of properties is available. In addition, the material properties of this graphite/epoxy system are representative of a class of commercially available graphite/epoxy materials.

Specimens

Sandwich beams such as the one shown in figure 1 were tested in this investigation. The specimens were 55.9 cm long by 7.6 cm wide and had a composite laminate on one face and a 0.32-cm-thick steel plate on the opposite face. The test laminates were supported on 2.5-cm-thick honeycomb core. Test specimens were loaded in four-point beam bending in order to get a uniform inplane stress field in a test area 7.6 by 7.6 cm in the center of the specimen. Two types of core, both of which had 0.32-cm cell size, were used in the impact area and they are indicated in table II along with the face-sheet materials and lamina orientation. The core materials were selected because they are commonly used in structural applications with the given test face sheet. Outboard from the center section a dense aluminum core was used where high shear loads occur in the beam.

The face-sheet laminates were cut from large panels which were cured according to the manufacturer's recommended cure cycle. Following cure the panels were inspected using an ultrasonic scanning technique, cut to size, and bonded to the honeycomb with a 395K-cure sheet adhesive.

Sandwich beams were selected for test in this investigation for two reasons. First, many secondary components on commercial transports are of sandwich construction; therefore, results of this investigation should be applicable directly

to the design of such structures. Second, these beams have high bending stiffness which eliminates the need to investigate the effect of specimen-impact load interactions which occur with large thin-gage panels supported at the boundary. Therefore, tests on these specimens should be representative of the worst-case design condition for composite laminates which may be subjected to impact damage.

APPARATUS AND TESTS

Apparatus

The apparatus used to propel the impact projectile is shown in schematic form in figure 2. Air is introduced slowly into the reservoir until the diaphragm ruptures. The air escapes through a metering orifice and propels the aluminum ball toward the target. A velocity detector is located near the end of the barrel. As the projectile passes through this area it interrupts light beams at two locations, which triggers electronic timing equipment to record the travel time between the beams. The velocity measuring apparatus is accurate to within ±3 percent.

Static loads were applied to the test specimens with the loading frame shown in figure 3. The specimen is loaded in the frame through a whiffletree arrangement connected to a screw jack in the rear. The loads on the beam are reacted by two support bars located near the end of the frame. Both loading and reaction supports are parallel and can pivot freely to alleviate extraneous inplane loads which might be imposed as the specimen bends. A load cell to measure the applied load was incorporated into the frame. The arrangement shown in figure 3 was used for compression testing; however, the same frame was also used in a slightly modified manner for tensile testing.

Tests

Tests were conducted to determine the effect of projectile impact and load on laminate strength. The sandwich-beam specimens were mounted in the frame and loaded to a fraction of the predetermined ultimate load. At that load the specimens were subjected to impact by a 1.27-cm-diameter spherical projectile. Specimens were tested under both tension and compression loading. Some specmens failed catastrophically upon impact while others incurred only local damage. The panels with local damage were then statically loaded to determine residual strength.

The impact projectile and velocity range (5.2 to 48.8 m/sec) were selected to simulate rock or hailstone-type damage. Rock damage is of interest because commercial aircraft are subjected to damage by rock and runway debris that is kicked up by tires and reverse thrusters. For tests in the velocity range of 15.9 to 48.8 m/s (0.37 to 3.5 J) 1.27-cm-diameter aluminum spheres with a mass of 2.9 grams were used as the impact projectile. Aluminum was chosen as the projectile material because it has about the same density as common rock materials. For impacts at velocities lower than 15.9 m/s, a 1.27-cm-diameter steel projectile was dropped on the test specimens. All impacts were at normal incidence.

RESULTS AND DISCUSSION

Tension-Loaded Laminates

The effect of low-velocity projectile impact on the strength of $[0/90]_S$ graphite/epoxy laminates loaded in tension is shown in figure 4. The ordinate is the static load P applied to the specimen prior to impact divided by the average ultimate load P_{ult} of several undamaged test specimens. The abscissa is the incident kinetic energy of the 1.27-cm-diameter projectile. Incident kinetic energy has been shown in reference 1 to provide good correlation for visible impact damage on the specimen surface. The filled symbols represent test specimens in which catastropic failure occurred due to projectile impact and the open symbols represent specimens which may have incurred local damage but did not fail catastrophically. The curve shown in figure 4 represents the lowest static load which precipitated catastrophic failure at a given impact energy level and is subsequently called the impact failure threshold. Also shown in figure 4 is the residual strength of the specimens which did not fail catastrophically upon impact. For most test specimens the residual strength exceeded the impact failure threshold which indicates that this threshold could be considered a reasonable estimate of the residual strength for panels damaged by impact. The lowest projectile kinetic energy at which surface-fiber failure can be detected visually is called the visible-damage threshold and is also indicated in figure 4. These data indicate that projectile impacts at energy levels below that which causes visible damage can initiate catastrophic failures in loaded composite structures. At impact energy levels greater than that which causes visible damage there is very little change in the impact failure threshold for this test laminate.

The data shown in figure 4 are typical of those for all laminates evaluated in this investigation although the failure-threshold curves were somewhat different for the different laminates. Failure-threshold curves for all test laminates are compared in figure 5. Basic test data used to obtain the failure-threshold curves of figure 5 are given in figure 6.

The failure-threshold curves for similar laminates are given together in figure 5 for comparison purposes. Also shown for comparison in figures 5(a) and 5(b) is the curve from figure 4 for the $[0/90]_S$ graphite/epoxy laminate. All data shown in figures 5(a) and 5(b) are for laminates supported on 48-kg/m^3 Nomex[2] honeycomb core while the data shown in figures 5(c) and 5(d) are for laminates supported on 130-kg/m^3 aluminum honeycomb core. All failure-threshold curves except the $[90/\pm45/0]_S$ Kevlar laminate approach asymptotic values between 40 to 50 percent of the undamaged ultimate strength. The failure-threshold curves for these laminates also approached asymptotic values at relatively low values of projectile kinetic energy. The data indicate that the difference in core substrate density has little effect on impact-initiated failures. For the graphite/epoxy laminates the effect of thickness, lamina orientation, or the incorporation of Kevlar has no appreciable effect on the damage tolerance of these tensile-stressed laminates. All of the graphite/epoxy dominated laminates had significant reductions in laminate strength. The $[90/\pm45/0]_S$ Kevlar lami-

[2]Nomex: Trade name of E. I. duPont de Nemours & Co., Inc.

nate was the most damage tolerant of all laminates tested in that it had the largest increase in load capability over its graphite/epoxy counterpart.

Photographs of several typical failed test specimens are shown in figure 7. Figures 7(a) and 7(b) are graphite/epoxy laminates that failed catastrophically on impact. The specimen shown in figure 7(a) is a $[0/90]_S$ laminate which sustained local damage at the impact site and initiated failure which progressed outward in a well-defined straight line. Specimens which had angle-ply lamina in the laminate (fig. 7(b)) experienced noticeably more delamination and fiber pull-out in failed panels.

Observation of failures in the hybrid specimens fabricated from a combination of graphite/epoxy and Kevlar/epoxy indicated that local failures were accompanied by delamination at the interface between the Kevlar and graphite. The size of the interface delaminations was dependent upon the velocity of the impact projectile. Typical examples can be observed in the photographs of figures 7(c) and 7(d). Both specimens were loaded to approximately $P/P_{ult} = 0.50$ when impact occurred. Both specimens had local fiber failures in the outer ply and associated fan-shaped delamination patterns. The variation of the delamination size with energy (velocity) suggests that the delamination may be associated with dynamic-stress wave effects or local interlaminar shear failures. Although this phenomenon may also occur in the all-graphite laminates it cannot be observed visually.

The specific strengths of all test laminates in the undamaged condition are shown in figure 8 as a function of specific modulus. Also shown in figure 8 are the asymptotic failure-threshold values for the test laminates along with the tensile ultimate strength of 2024-T3 aluminum. The specific moduli shown in the figure are calculated values based on the material properties shown in table I. The significant reduction in strength due to impact, which was shown in previous figures, is also evident in this figure. These data indicate that, based on the failure threshold, all test laminates have a specific tensile strength equal to or greater than 2024-T3 aluminum. Indicated in the figure for reference purposes are lines of constant strain. On a strain basis, all filament-controlled graphite laminates (i.e., laminates with 0° graphite lamina) fail at an undamaged ultimate strain near 0.011. These same laminates fail due to impact damage at strains between 0.004 and 0.006. The two Kevlar laminates tested were also filament controlled and failed at an undamaged ultimate strain of 0.018. These same laminates failed due to impact damage at strains near 0.011. These data indicate that for filament-controlled laminates loaded in tension strain is a good indicator of laminate performance, both in the undamaged as well as the damaged condition.

Compression-Loaded Laminates

The effect of low-velocity impact on the compression strength of $[0/90]_S$ graphite/epoxy test specimens is shown in figure 9. The abscissa and ordinate of this figure are the same as those used in previous figures for the tension-loaded laminates. These data indicate that the compression-loaded laminates exhibited the same basic character as the tension-loaded laminates. This behavior was not expected because most common materials used for the fabrication

of aerospace structures do not exhibit unstable crack propagation under compression loading. It is also of interest to note that projectile impact at energy levels below the visible damage threshold is capable of initiating catastrophic failures in compression-loaded laminates. The impact-failure-threshold curve for this compression-damaged laminate does not reach an asymptotic value as rapidly as the tension threshold curves.

All laminates evaluated in this investigation under compression loading exhibited the same basic behavior as the data shown in figure 9 although the impact-failure-threshold curves were somewhat different for the different laminates. Failure-threshold curves for all compression test laminates are shown in figure 10 for comparison purposes. Test data similar to that shown in figure 9 were used to obtain the failure-threshold curves and these data are given in figure 11. The data of figure 10 indicate that the hybrid laminate does significantly improve the damage tolerance when compared to the all-graphite $[0/90]_S$ laminate. This improvement was not anticipated particularly since Kevlar has a very low compression strength. Close examination of the failure surface indicates that impact precipitates a transverse shear-type failure in compression-loaded graphite laminates similar to that shown in sketch (a). Transverse shear failures in the graphite lamina of a hybrid specimen are suppressed by the outer plies of the Kevlar resulting in improved impact performance.

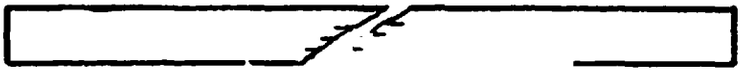

Sketch (a)

The failure modes in compression were similar to those observed in tension. The $[0/90]_S$ laminate compression failure, for example, was nearly identical to the tensile failure shown in figure 7(a) except there was some "brooming" which probaby occurred after the failure surface closed. Several of the thicker, heavily loaded laminates, had large chunks of material broken out of the specimen at failure. One such specimen is shown in figure 12.

The variations of specific strength with specific modulus of all compression-loaded laminates tested are compared in figure 13 on the same basis as the tensile data shown previously in figure 8. These data (fig. 13) indicate that based on the failure threshold several of the test laminates have a lower specific compression strength than 2024-T3 aluminum. Some laminates failed at strains below 0.004 which indicates that the degradation by impact in compression-loaded laminates is more severe than in tension-loaded laminates.

CONCLUSIONS

An experimental program evaluated the effect of impact on the tensile and compressive strengths of several graphite/epoxy and Kevlar 49/epoxy laminates. From the results of this investigation the following conclusions can be drawn:

1. Projectile impacts at energy levels below the visible-damage threshold initiated catastrophic failure in all test laminates loaded in either tension or compression.

2. Degradation in strength due to impact was more severe in some laminates loaded in compression than the same laminates loaded in tension.

3. The residual strength of specimens with local damage, in most cases exceeded the impact failure threshold, which indicates that this threshold could be considered a reasonable estimate of the residual strength for panels damaged by impact.

4. The consistency of the ultimate strain values for filament-controlled laminates loaded in tension indicates that laminate strain is a good indicator of laminate strength in the undamaged as well as the damaged condition.

5. The use of other materials such as Kevlar 49 to form graphite hybrids did not improve the impact resistance of laminates loaded in tension; however, there was improvement in some laminates loaded in compression.

Langley Research Center
National Aeronautics and Space Administration
Hampton, VA 23665
August 15, 1978

REFERENCES

1. Rhodes, Marvin D.: Low Velocity Impact on Composite Sandwich Structures. Proceedings of the Second Conference on Fibrous Composites in Flight Vehicle Design, AFFDL-TR-74-103, U.S. Air Force, Sept. 1974, pp. 275-298.

2. Rhodes, Marvin D.: Impact Fracture of Composite Sandwich Structures. AIAA Paper 75-748, May 1975.

TABLE I.- ELASTIC PROPERTIES OF LAMINA

Material	Ply thickness, cm	Modulus, GPa			Major Poisson ratio	Density, kg/m^3
		In fiber direction, E_{11}	Transverse to fiber, E_{22}	Shear, G_{12}		
Tension						
Graphite tape	0.0140	146.8	10.9	6.4	0.38	1520
181-style balanced graphite fabric	.0356	62.7	62.7	4.5	.10	1520
Kevlar tape	.0140	75.8	5.5	2.1	.34	1380
120-style balanced Kevlar fabric	.0114	31.0	31.0	2.1	.10	1380
181-style balanced Kevlar fabric	.0229	31.0	31.0	2.1	.10	1380
Compression						
Graphite tape	0.0140	131.0	13.0	6.4	0.38	1520
181-style balanced graphite fabric	.0356	62.7	62.7	4.5	.10	1520
Kevlar tape	.0140	75.8	5.5	2.1	.34	1380

TABLE II.- TEST SPECIMENS

Specimen type	Face-sheet material	Lamina orientation (a)	Honeycomb core in test area
1	Graphite tape	$[0/90]_S$	48-kg/m^3 Nomex
2	181-style graphite fabric	$[0_2]_T$	↓
3	Kevlar tape	$[0/90]_S$	
4	Hybrid	$[0_K/90_G/0_G]_S$	
5	Hybrid	$[0_{KA}/90_G/0_G]_S$	
6	Hybrid	$[0_{KB}/90_G/0_G]_S$	
7	Graphite tape	$[\pm60/0]_S$	130-kg/m^3 aluminum
8	Graphite tape	$[90/\pm45/0]_S$	↓
9	Kevlar tape	$[90/\pm45/0]_S$	
10	Graphite fabric and tape	$[45_{GB}/(0_G)_4]_S$	
11	Graphite tape	$[45/0/-45/0]_S$	↓

[a] G - Graphite tape
GB - 181-style graphite fabric
K - Kevlar tape
KA - 120-style Kevlar fabric
KB - 181-style Kevlar fabric

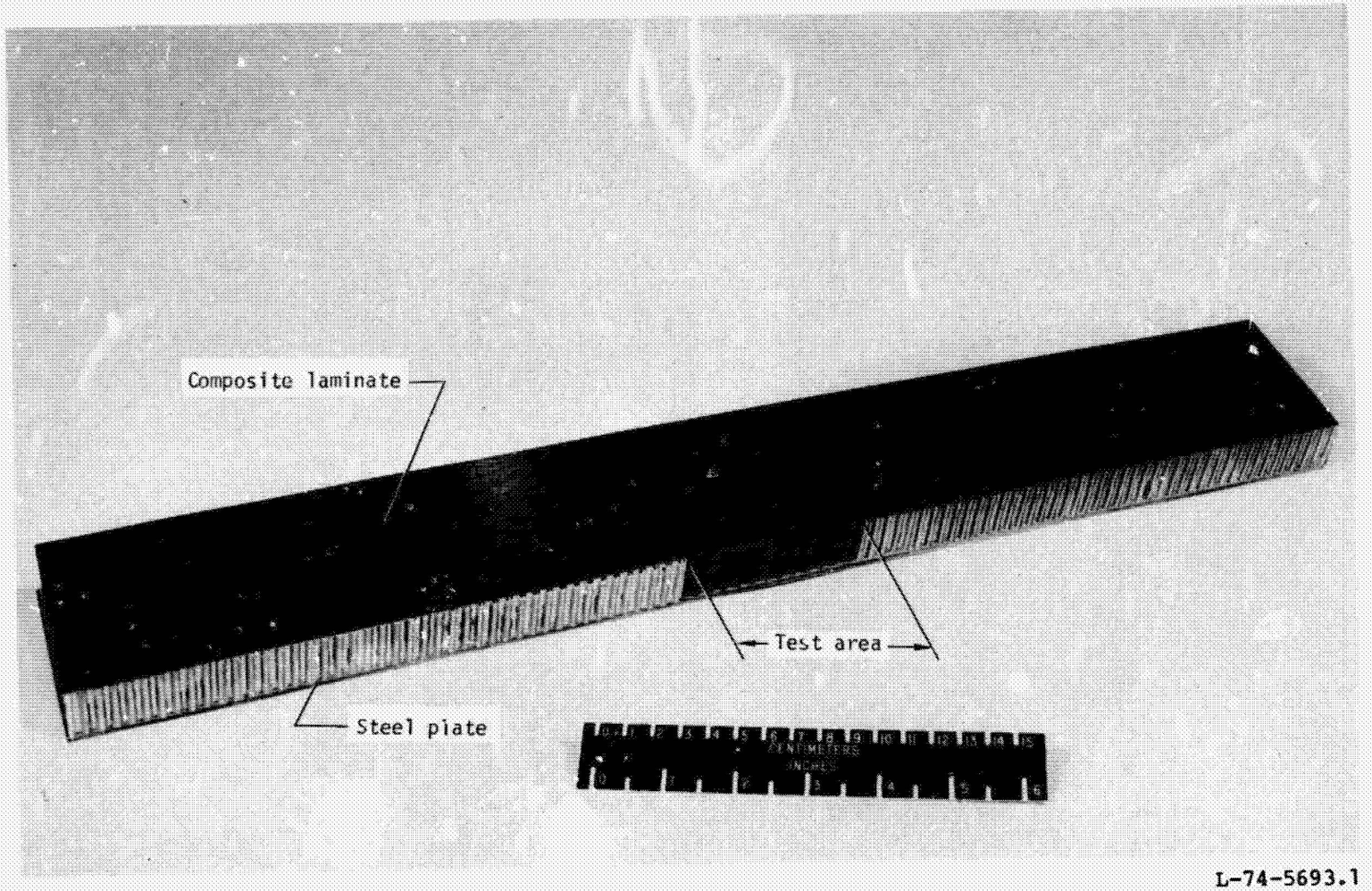

L-74-5693.1

Figure 1.- Typical test specimen.

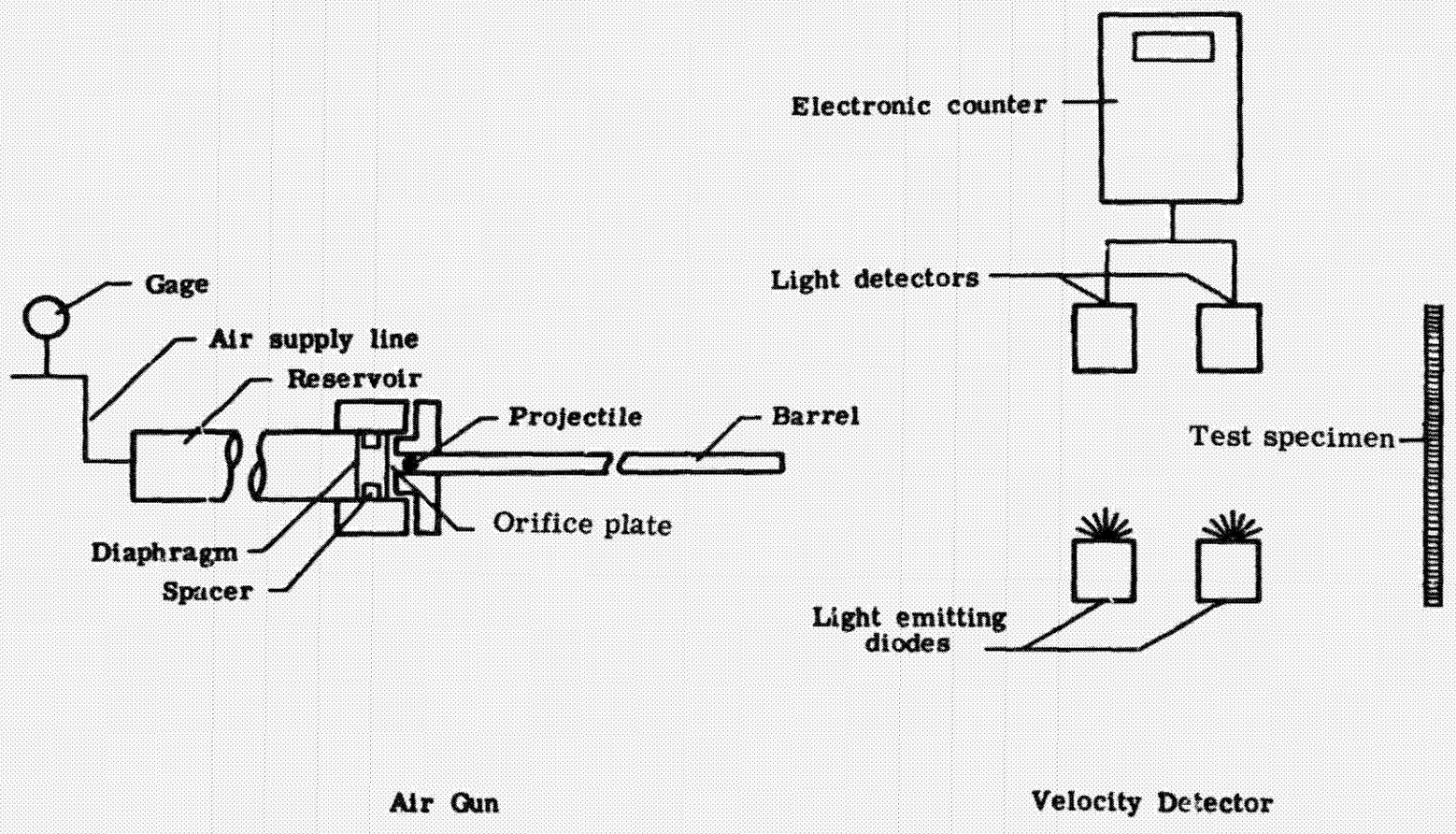

Figure 2.- Schematic drawing of air gun and velocity detector.

L-75-1483

Figure 3.- Frame used to apply static loads to the test specimens.

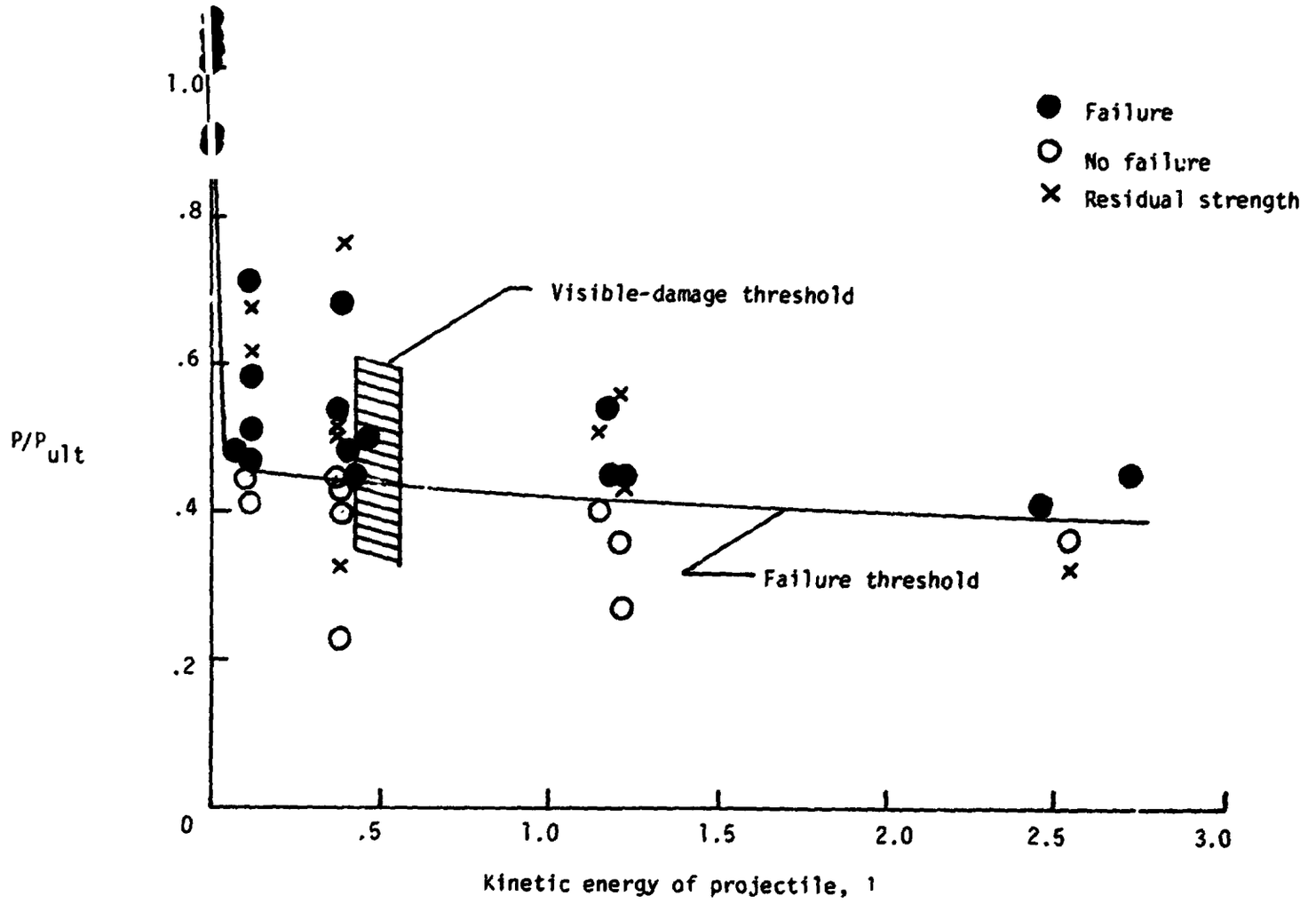

Figure 4.- The effect of impact on the tensile strength of the $[0/90]_S$ graphite/epoxy test laminate.

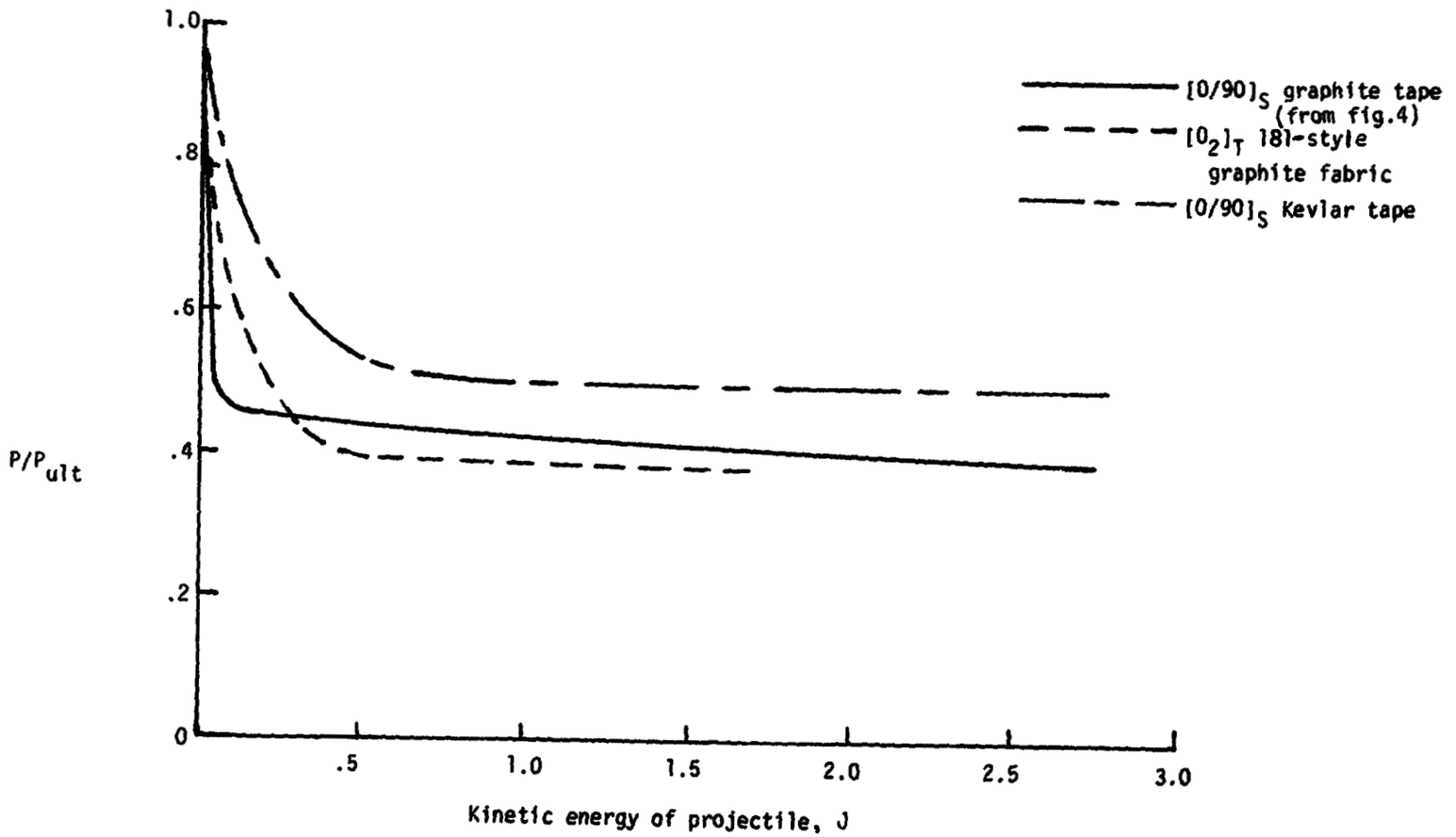

(a) Basic material laminates on 48-kg/m^3 Nomex honeycomb core.

Figure 5.- Failure-threshold curves for tension-loaded test laminates.

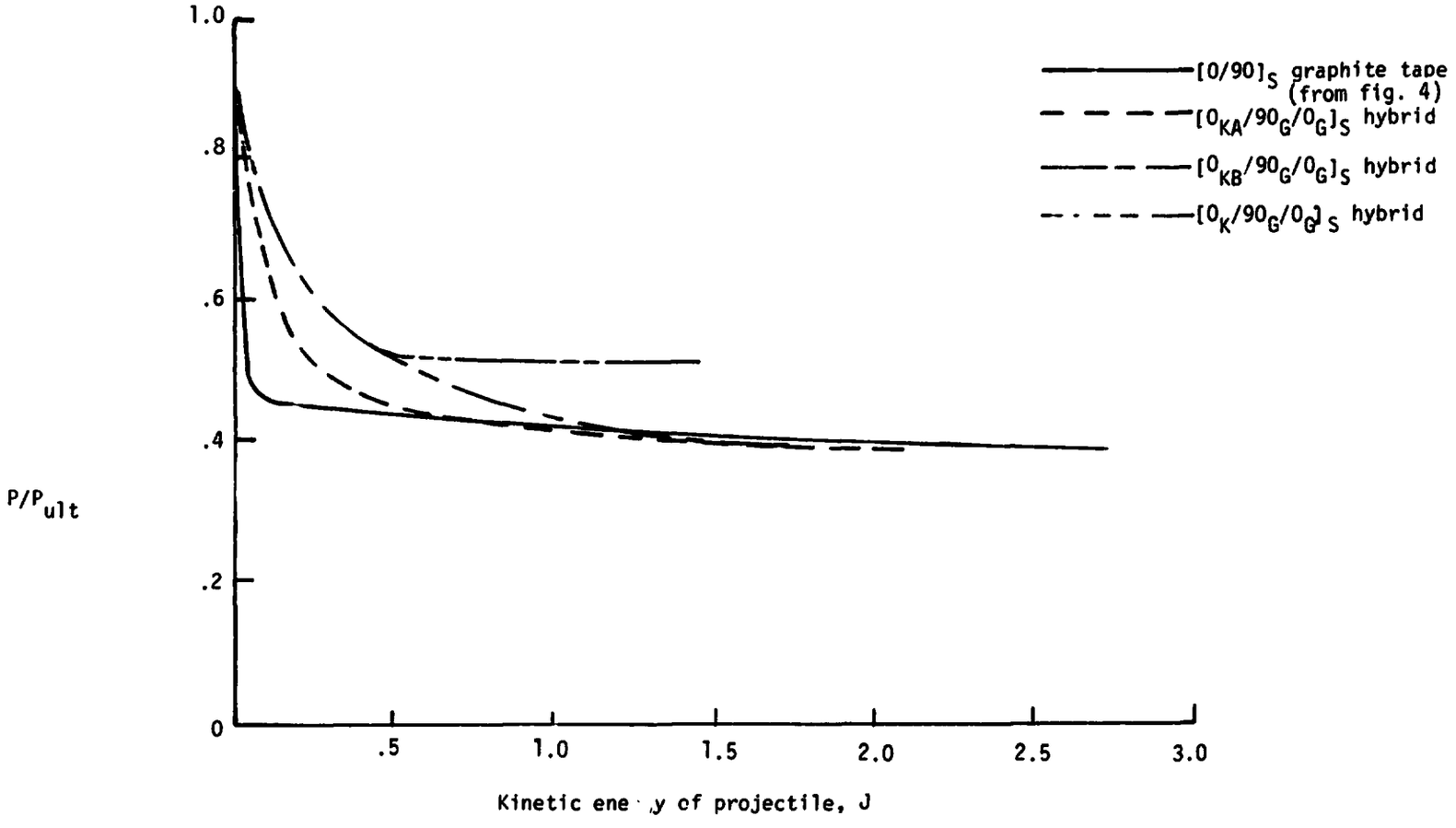

(b) Hybrid material laminates on 48-kg/m^3 Nomex honeycomb core.

Figure 5.- Continued.

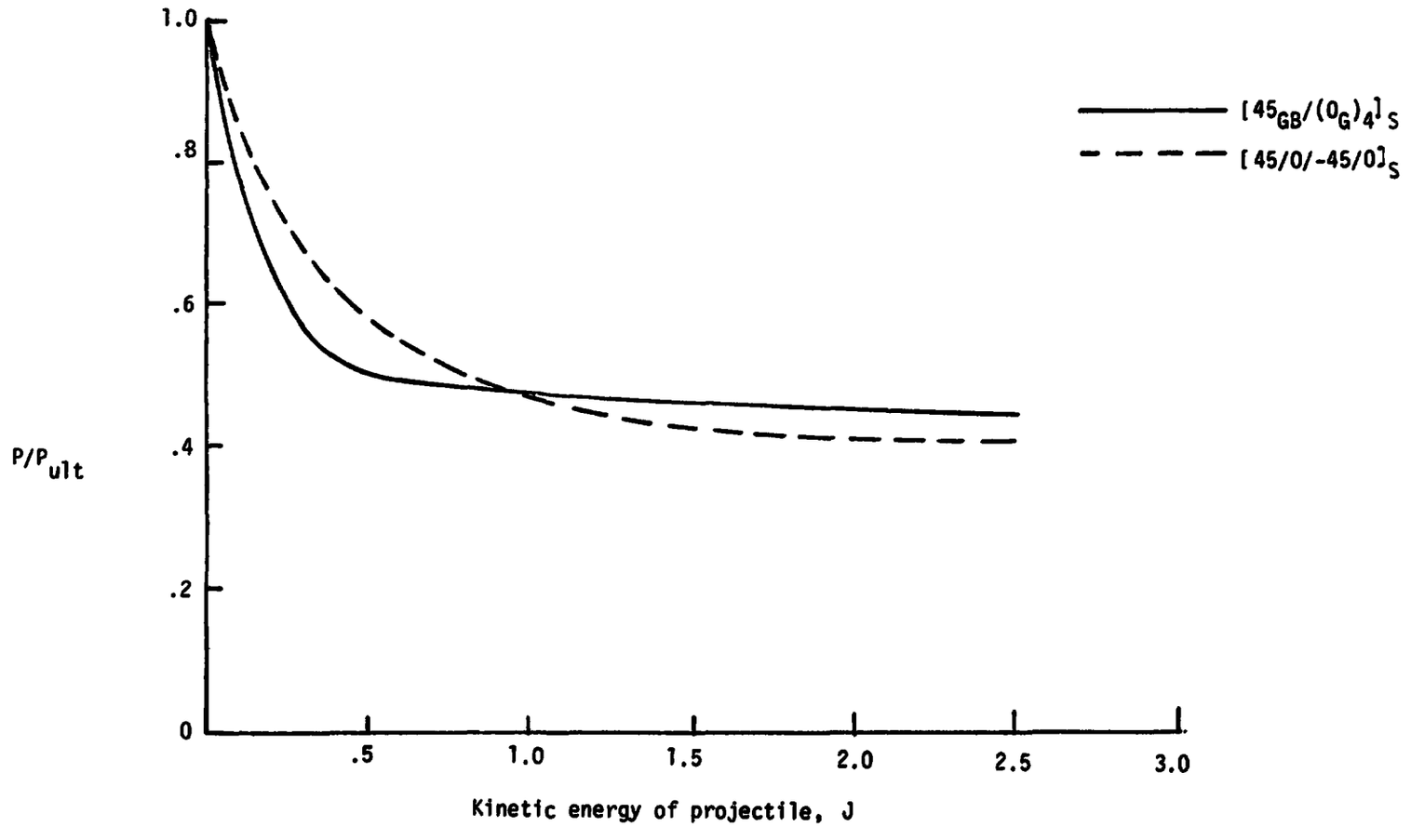

(c) Graphite/epoxy laminates on 130-kg/m^3 aluminum honeycomb core.

Figure 5.- Continued.

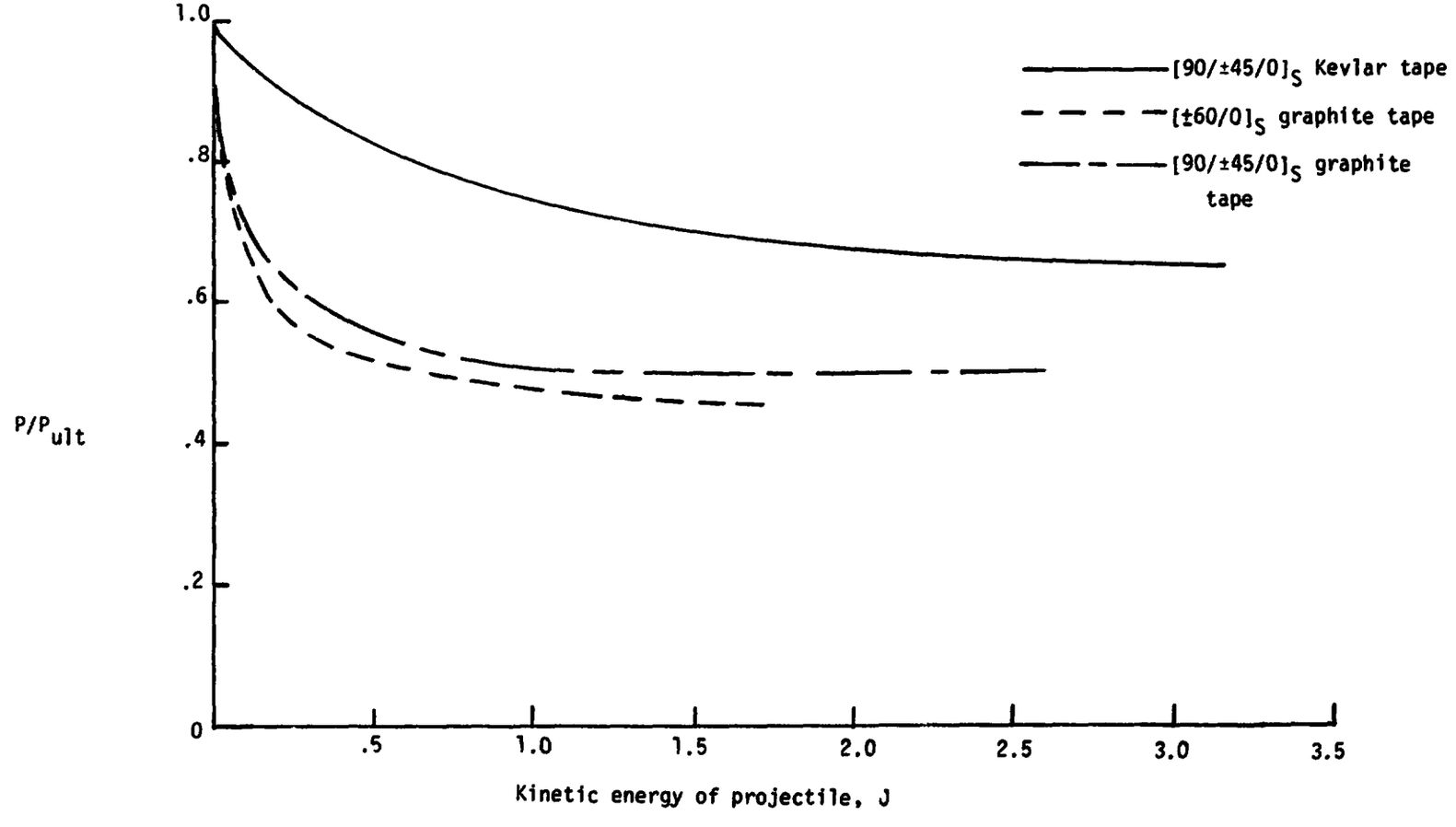

(d) Pseudoisotropic laminates on 130-kg/m^3 aluminum honeycomb core.

Figure 5.- Concluded.

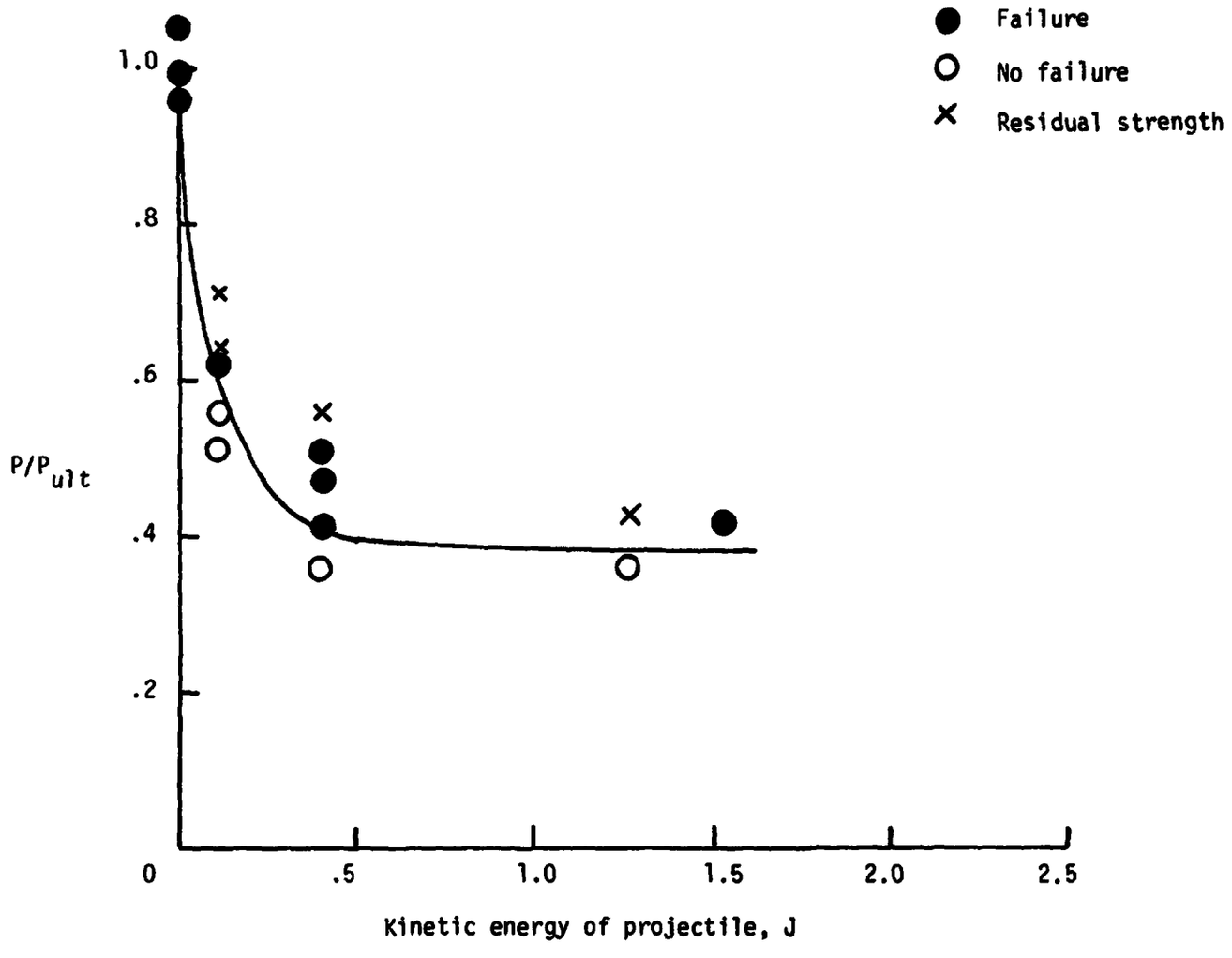

(a) $[0_2]_T$ 181-style graphite fabric.

Figure 6.- The effect of impact on the tensile strength of various test laminates.

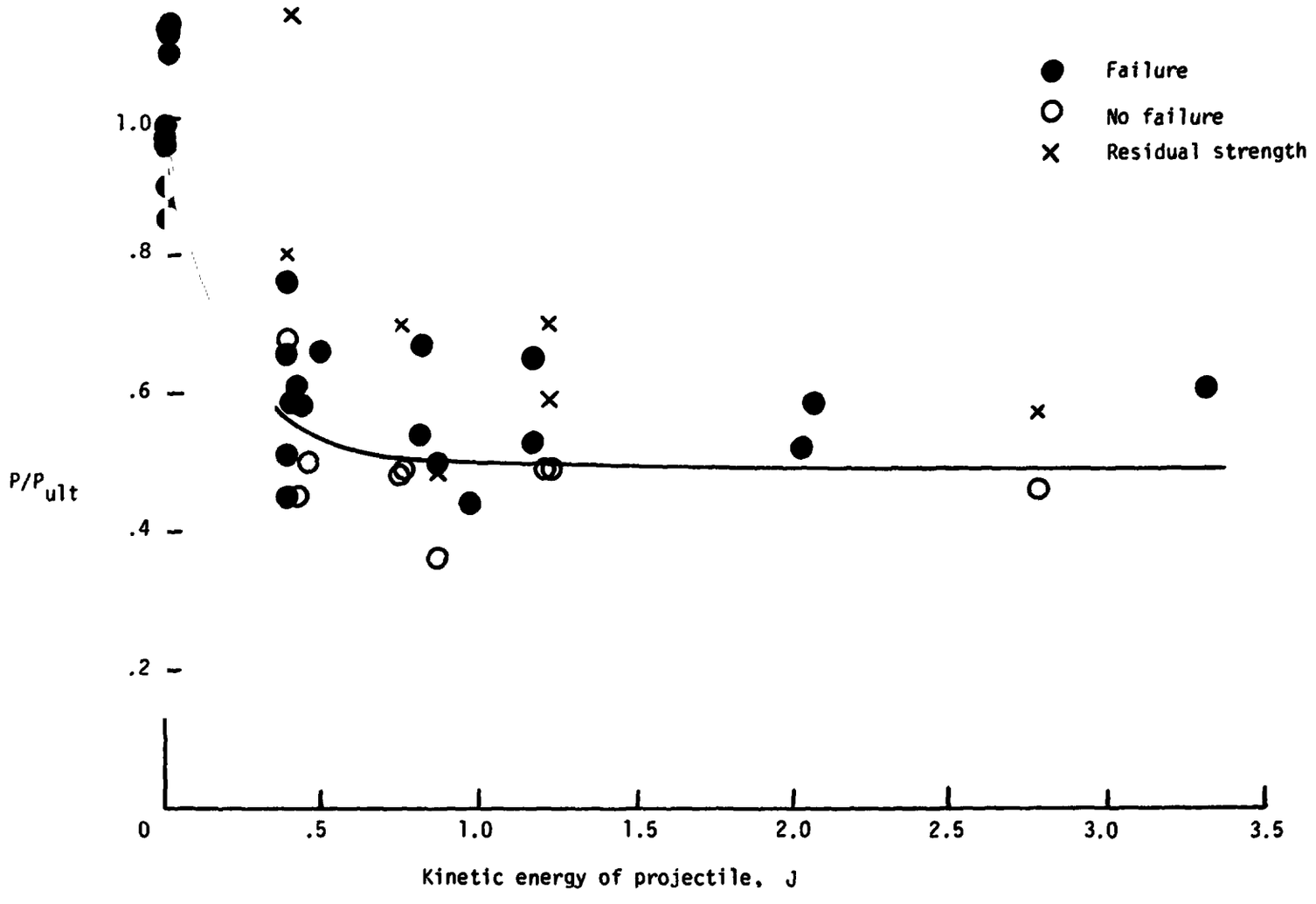

(b) $[0/90]_S$ Kevlar tape.

Figure 6.- Continued.

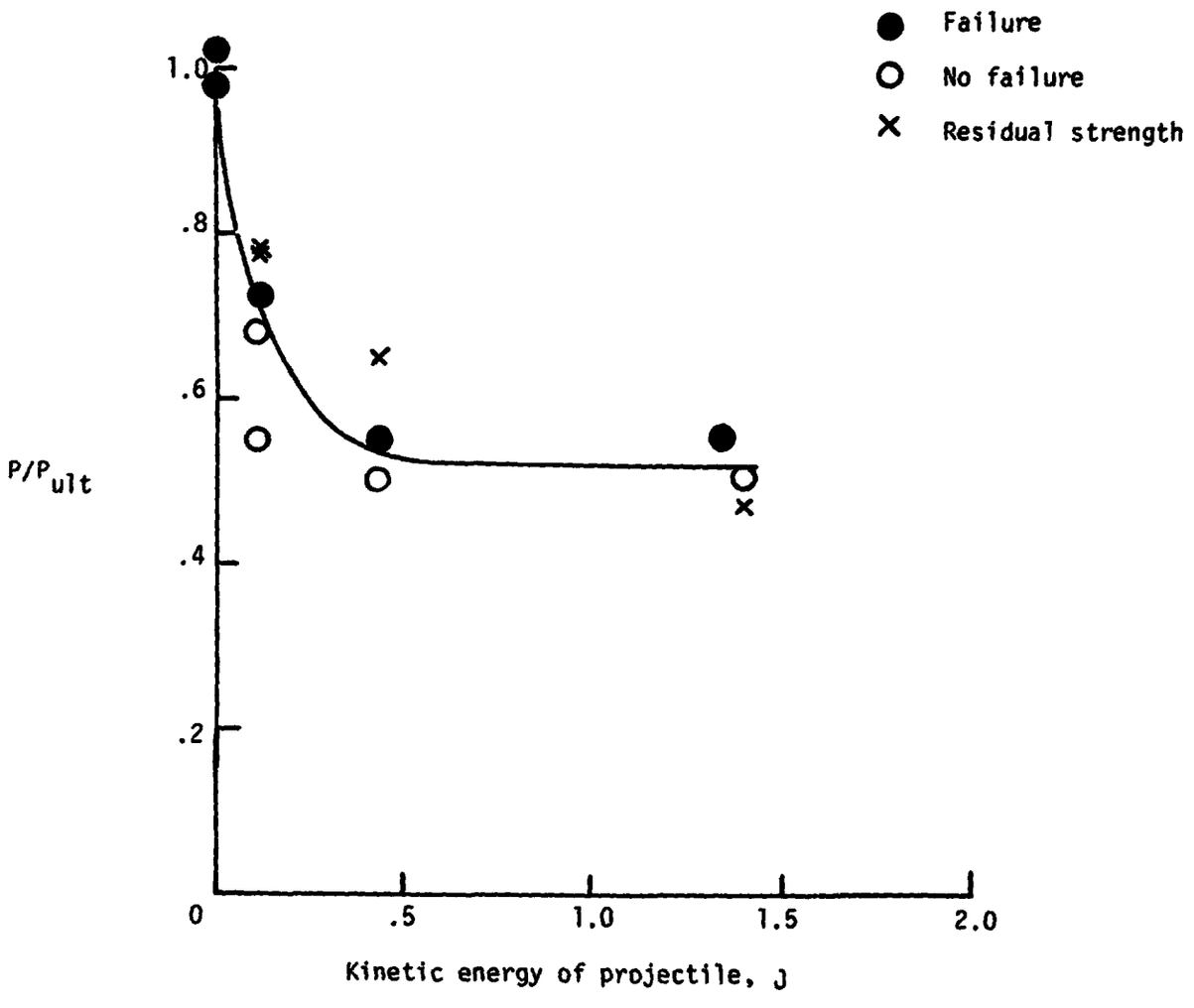

(c) $[0_K/90_G/0_G]_S$ hybrid of Kevlar and graphite tapes

Figure 6.- Continued.

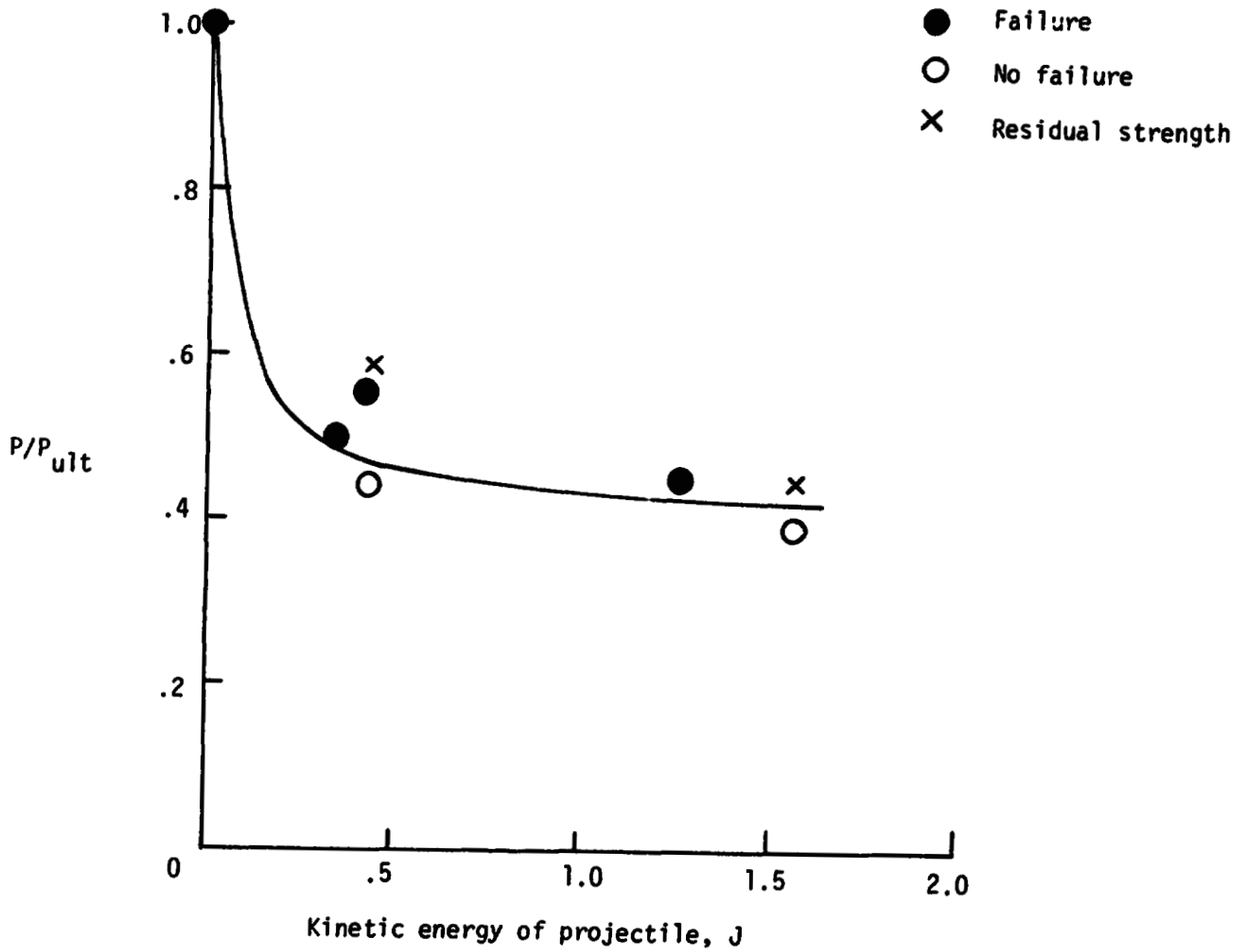

(d) $[0_{KA}/90_G/0_G]_S$ hybrid of 120-style Kevlar fabric and graphite tape.

Figure 6.- Continued.

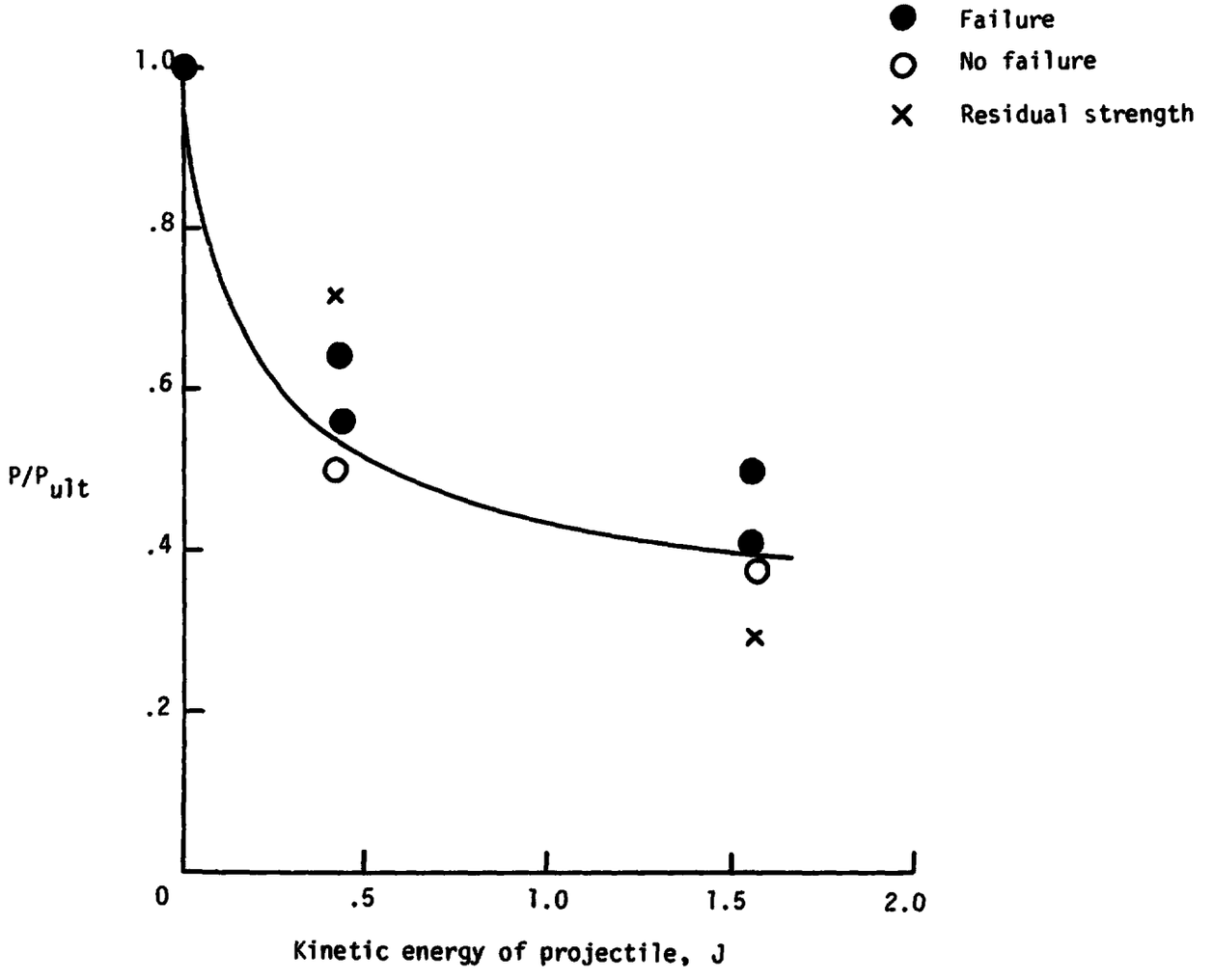

(e) $[0_{KB}/90_G/0_G]_S$ hybrid of 181-style Kevlar fabric and graphite tape.

Figure 6.- Continued.

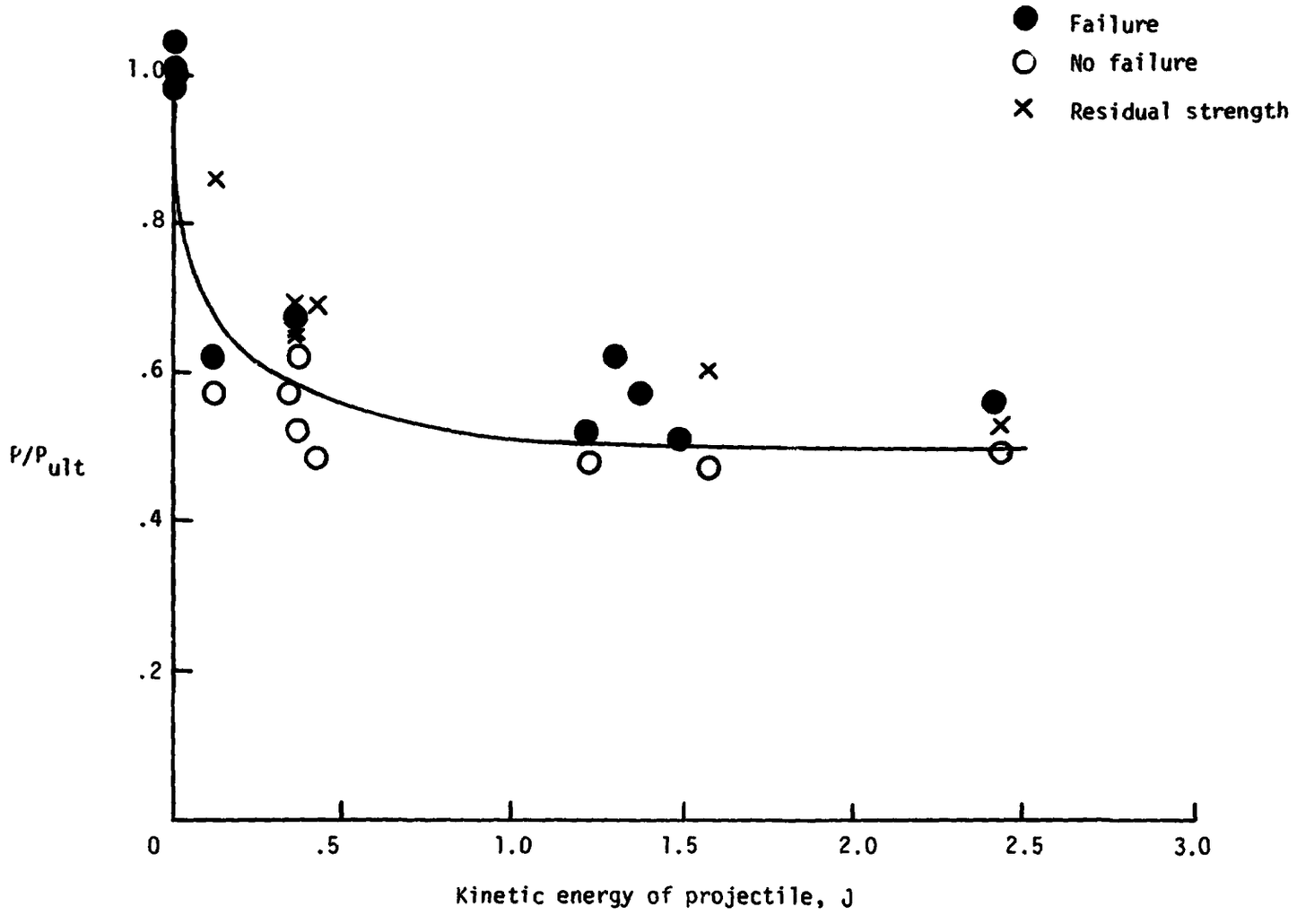

(f) $[\pm 60/0]_S$ graphite tape.

Figure 6.- Continued.

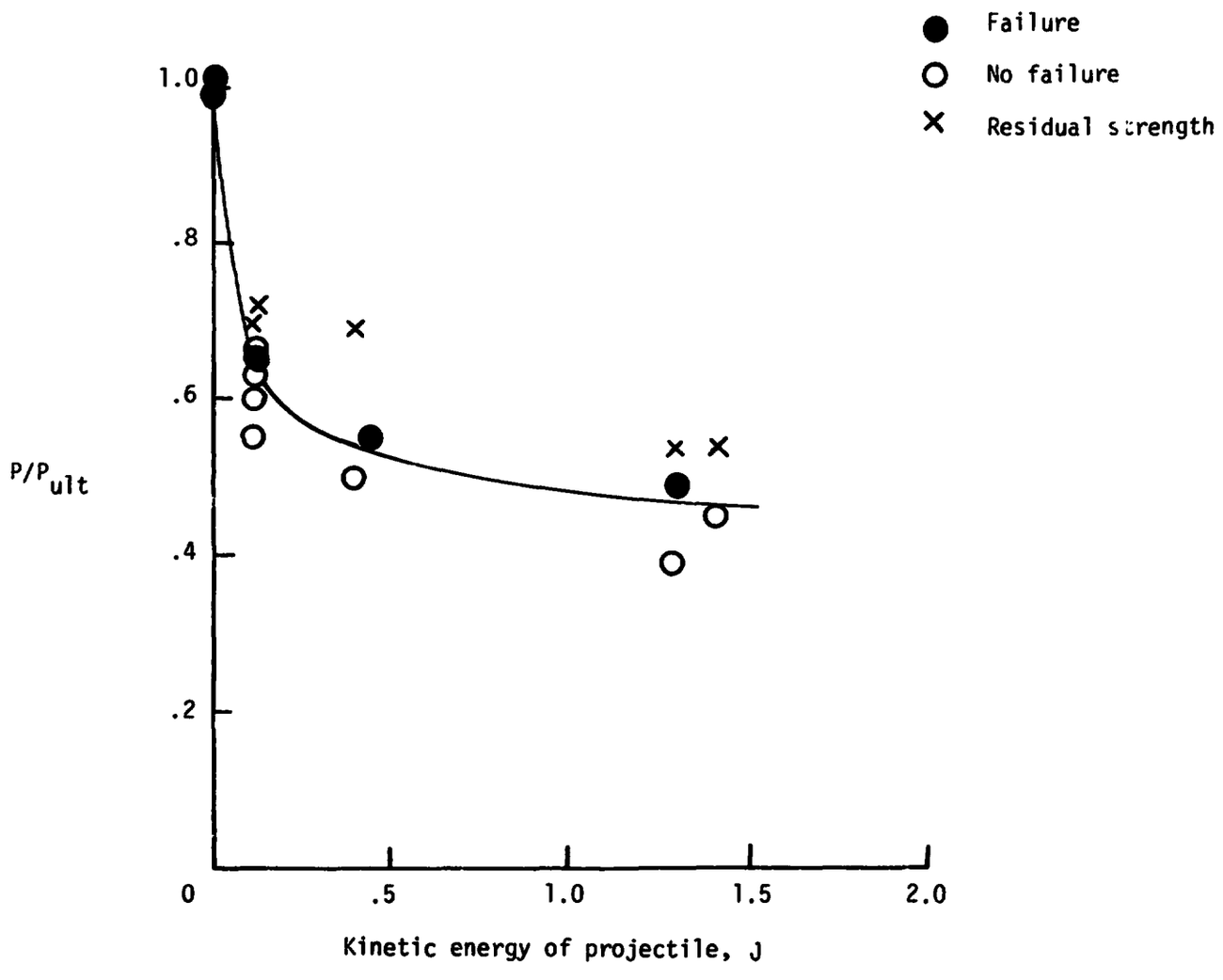

(g) $[90/\pm45/0]_S$ graphite tape.

Figure 6.- Continued.

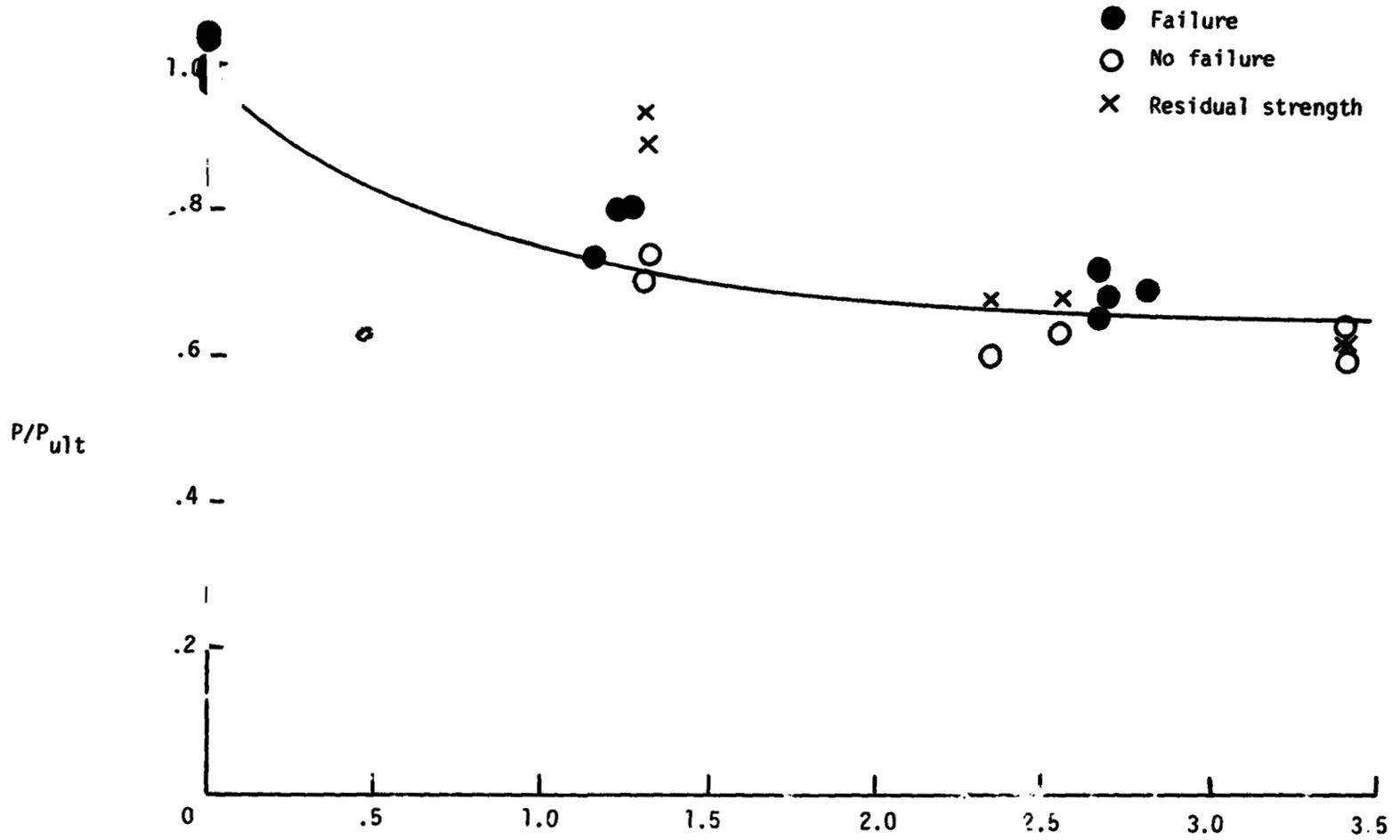

(h) $[90/\pm45/0]_S$ Kevlar tape.

Figure 6.- Continued.

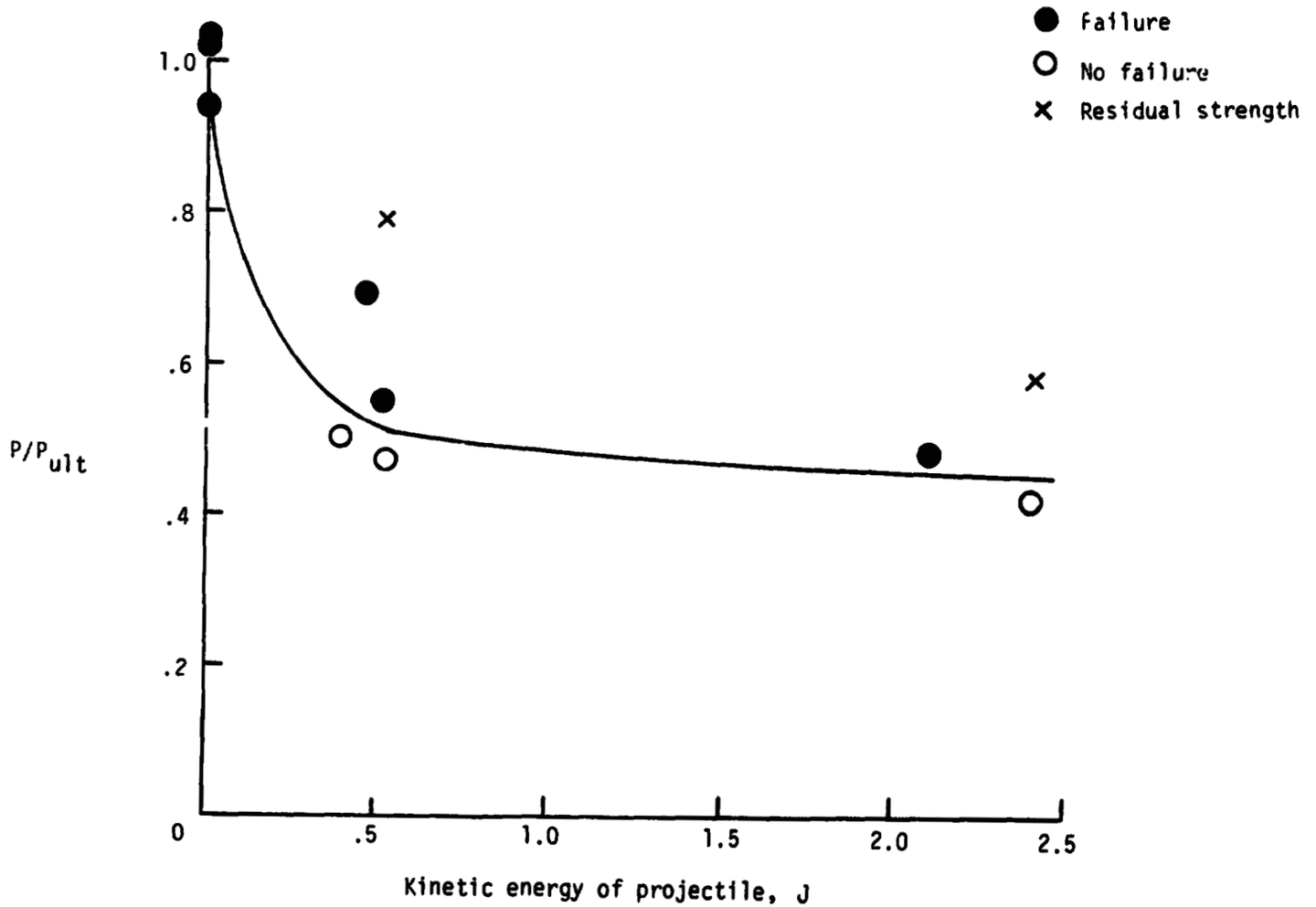

(i) $[45_{GB}/(0_G)_4]_S$ hybrid of 181-style graphite fabric graphite tape.

Figure 6.- Continued.

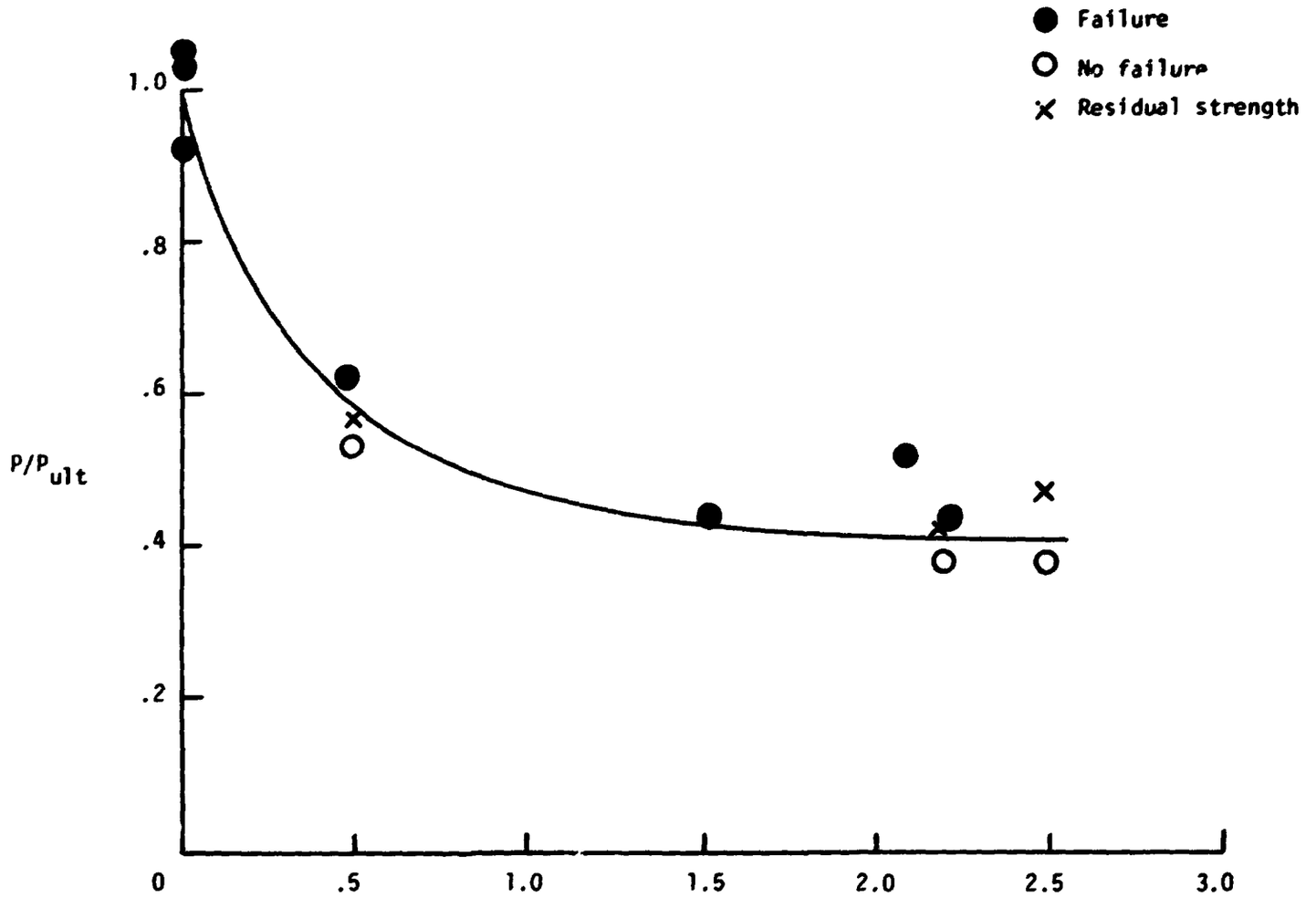

(j) $[45/0/-45/0]_s$ graphite tape.

Figure 6.- Concluded.

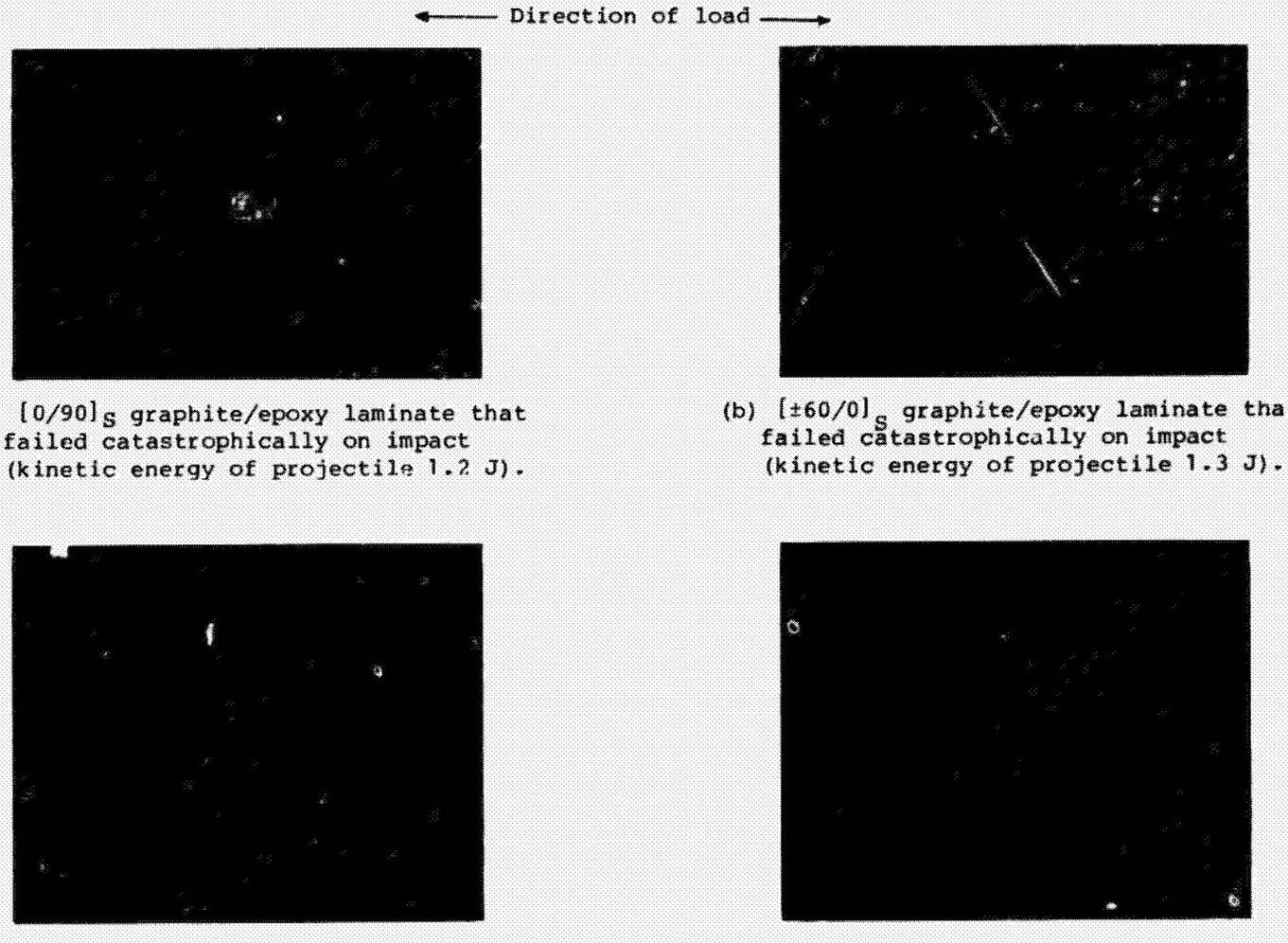

(a) $[0/90]_S$ graphite/epoxy laminate that failed catastrophically on impact (kinetic energy of projectile 1.2 J).

(b) $[\pm 60/0]_S$ graphite/epoxy laminate that failed catastrophically on impact (kinetic energy of projectile 1.3 J).

(c) $[0_K/90_G/0_G]_S$ hybrid laminate that sustained local damage on impact (kinetic energy of projectile 0.4 J).

(d) $[0_K/90_G/0_G]_S$ hybrid laminate that sustained local damage on impact (kinetic energy of projectile 1.4 J).

L-78-116

Figure 7.- Photographs of several test specimens which were statically loaded in tension at the time of impact.

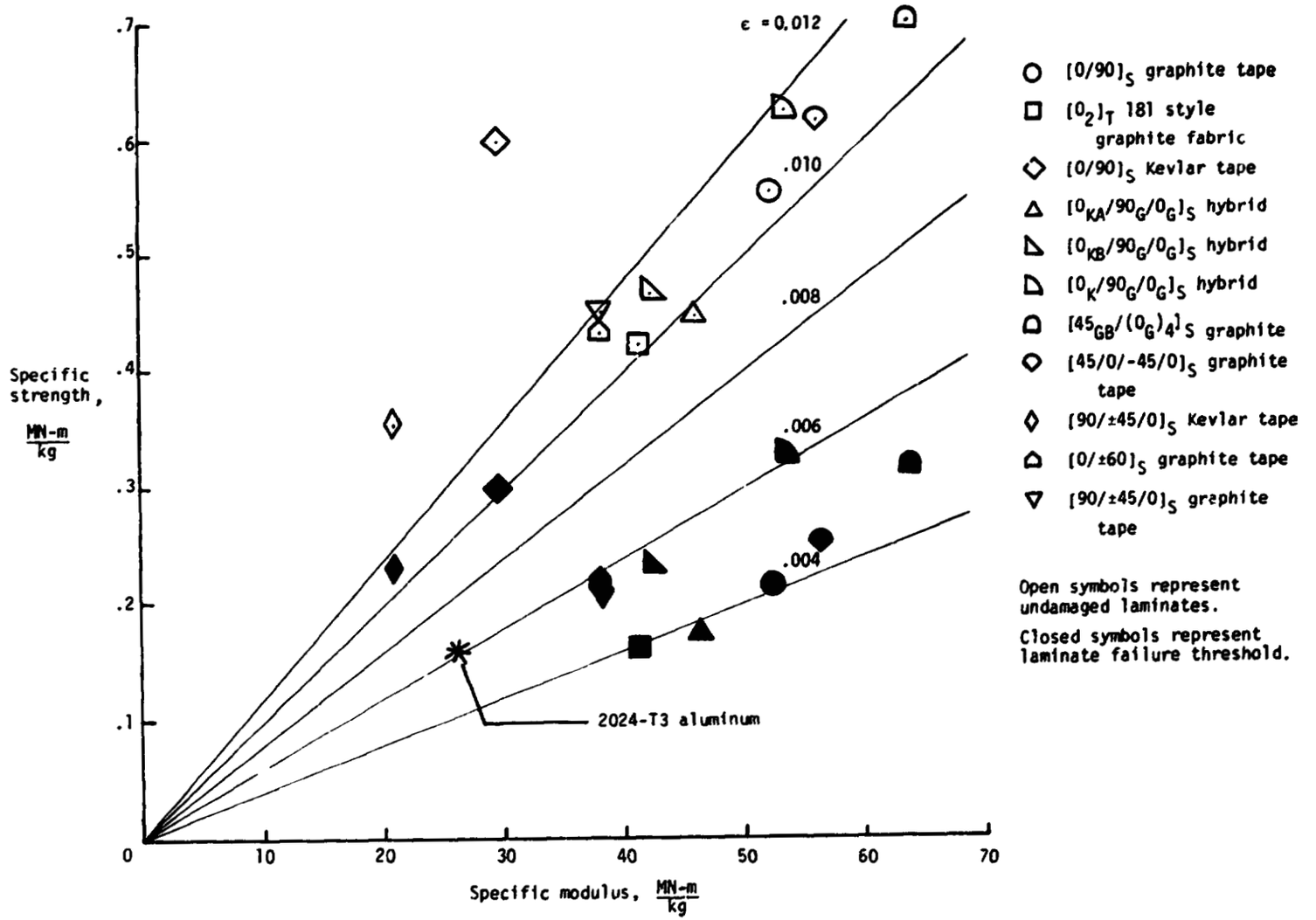

Figure 8.- Specific tensile strength as a function of specific tensile modulus of test laminates in the undamaged condition and at the failure threshold, compared with a typical aluminum.

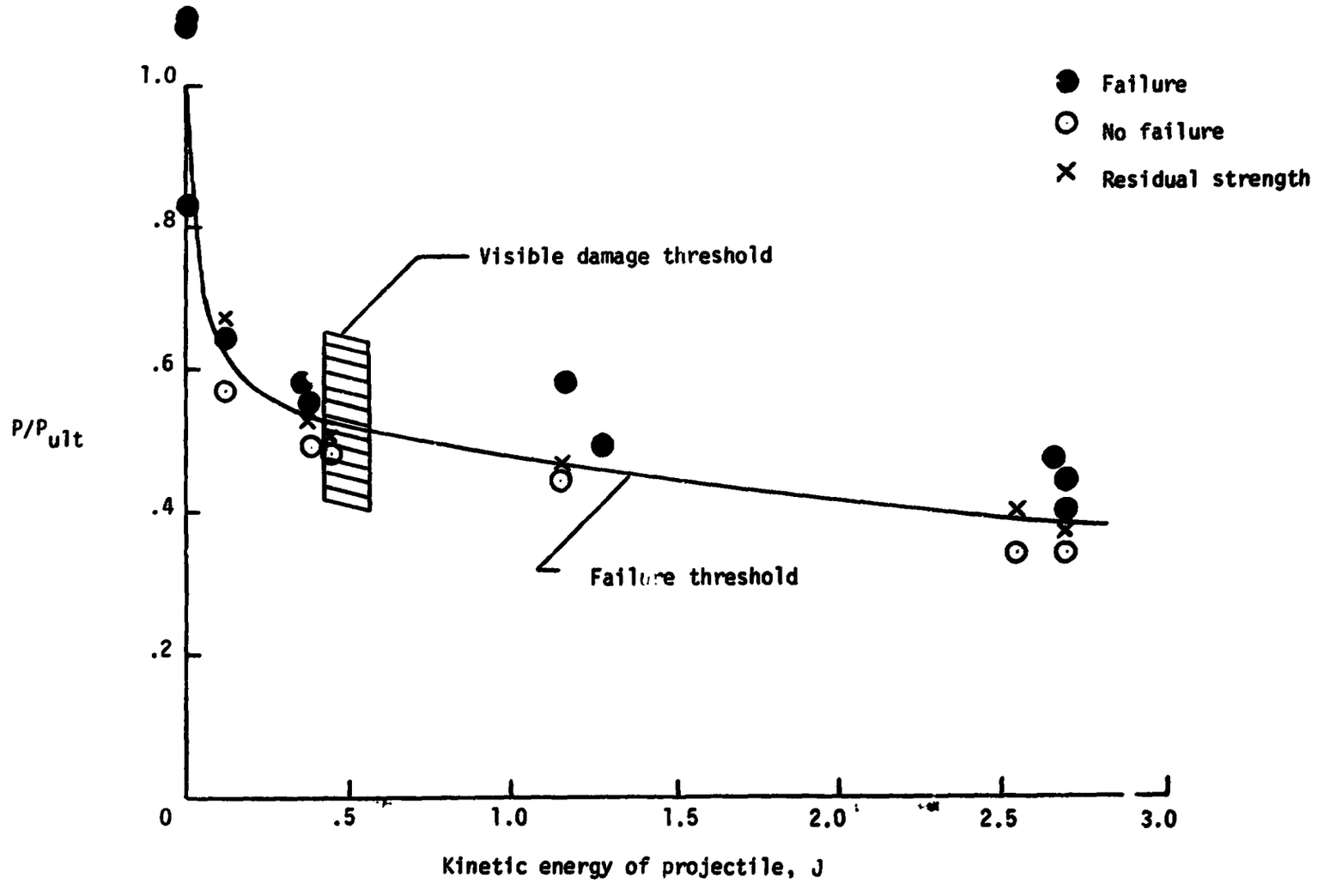

Figure 9.- The effect of impact on the compression strength of the $[0/90]_s$ graphite/epoxy test laminate.

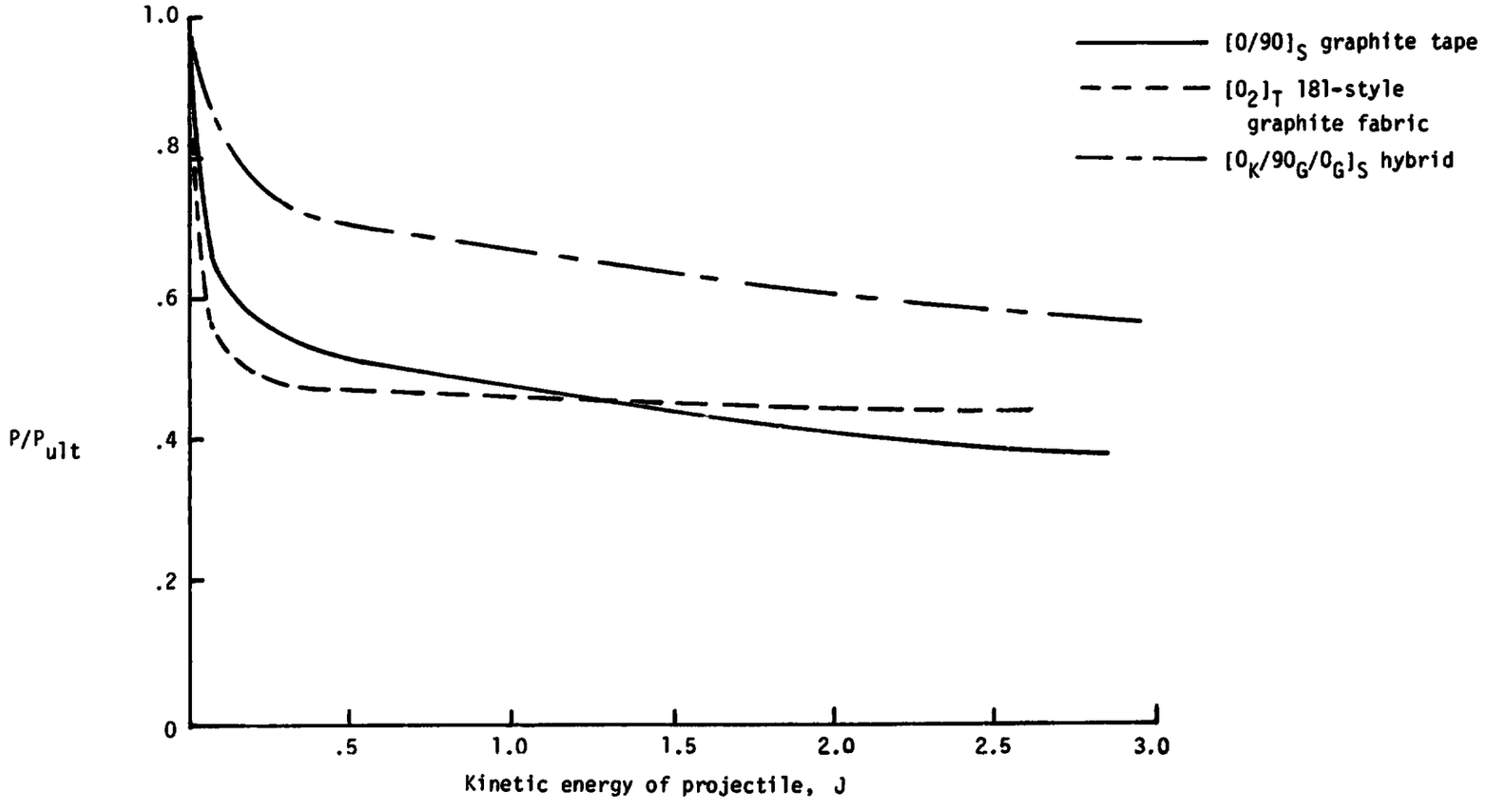

(a) Basic material laminates on 48-kg/m^3 Nomex honeycomb core.

Figure 10.- Failure-threshold curves for compression-loaded test laminates.

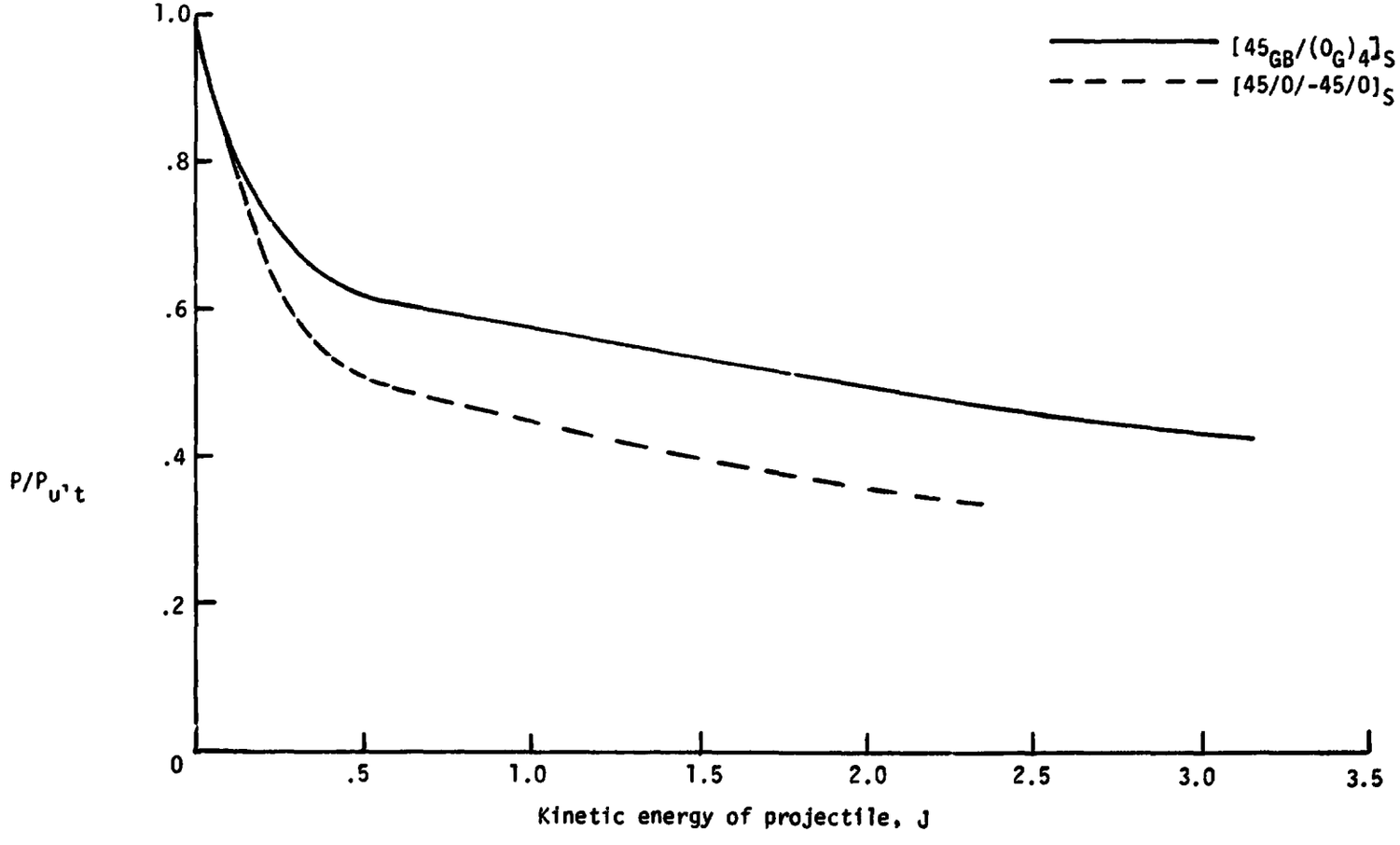

(b) Graphite/epoxy laminates on 130-kg/m^3 aluminum honeycomb core.

Figure 10.- Continued.

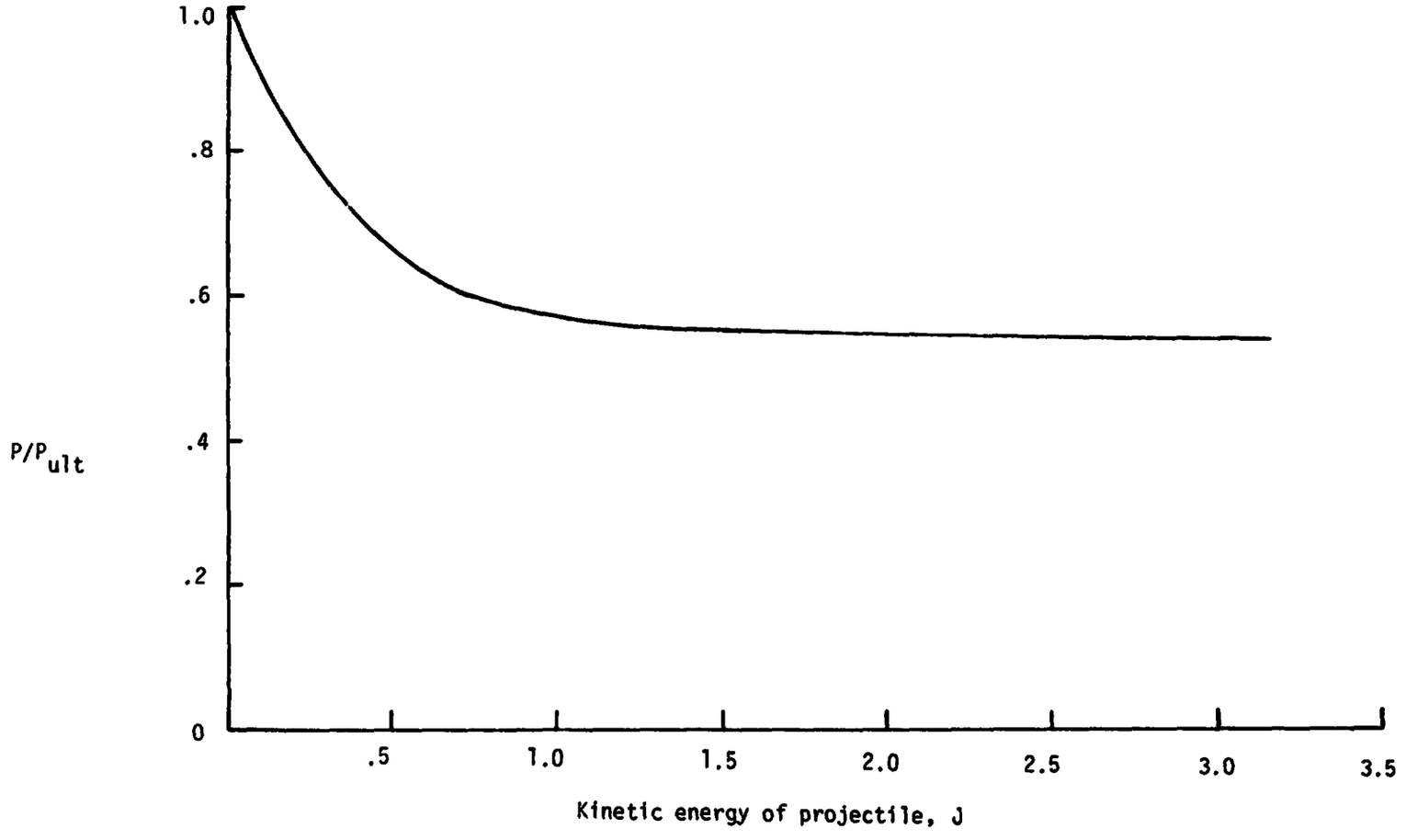

(c) $[90/\pm45/0]_S$ graphite/epoxy on 130-kg/m^3 aluminum honeycomb core.

Figure 10.- Concluded.

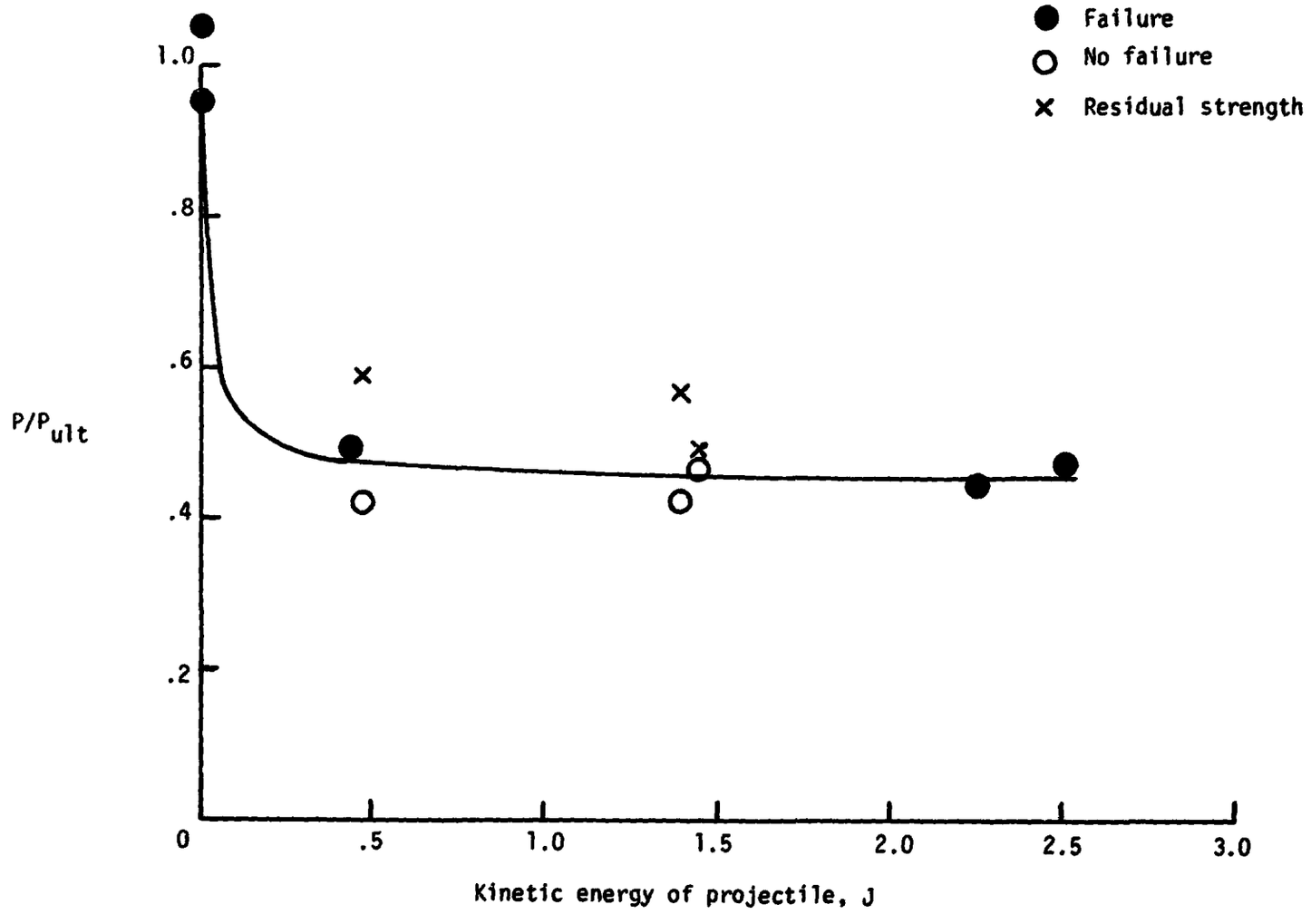

(a) $[0_2]_T$ 181-style graphite fabric.

Figure 11.- The effect of impact on the compression strength of test laminates.

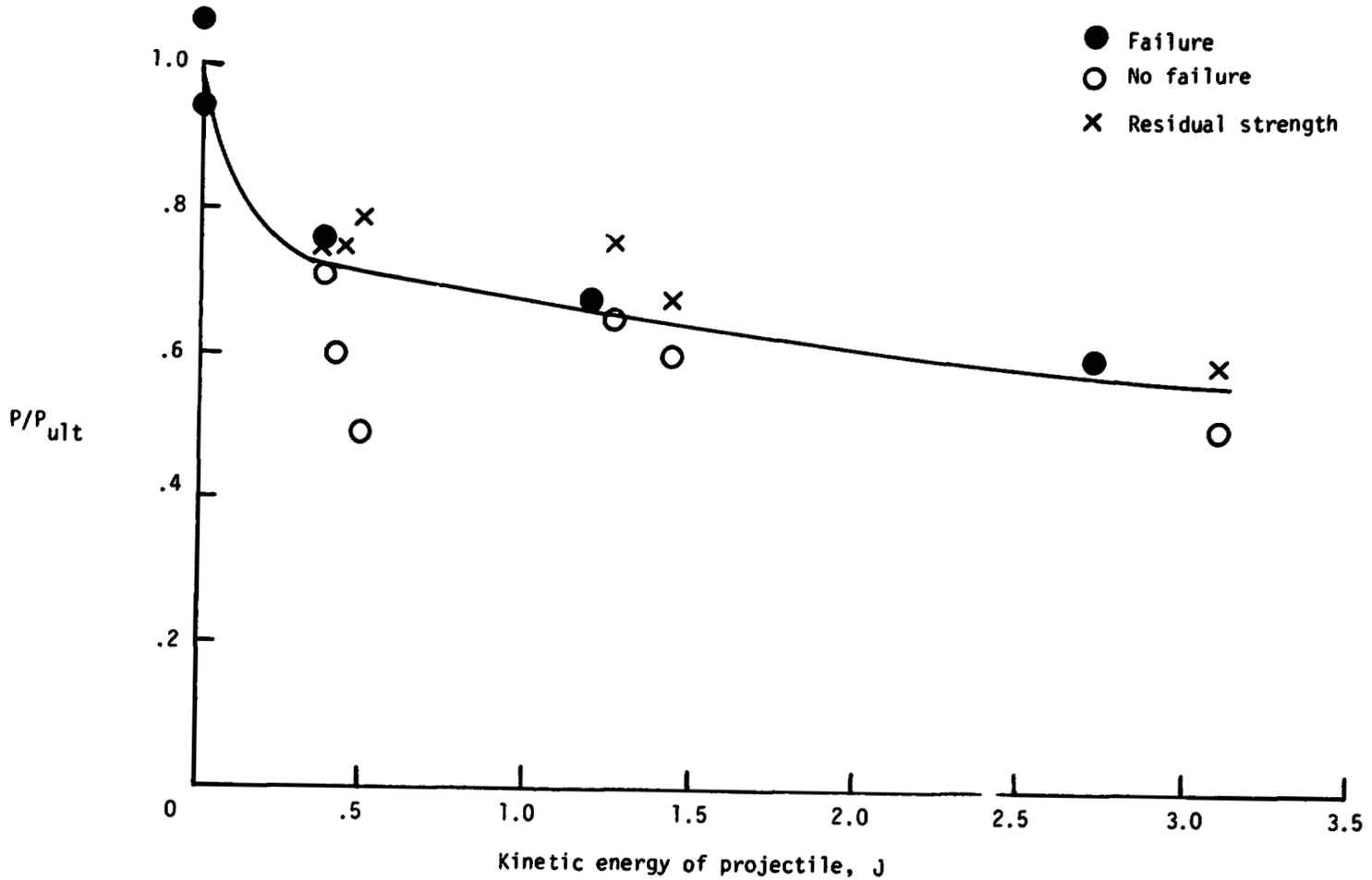

(b) $[0_K/90_G/0_G]_S$ hybrid of Kevlar and graphite tapes.

Figure 11.- Continued.

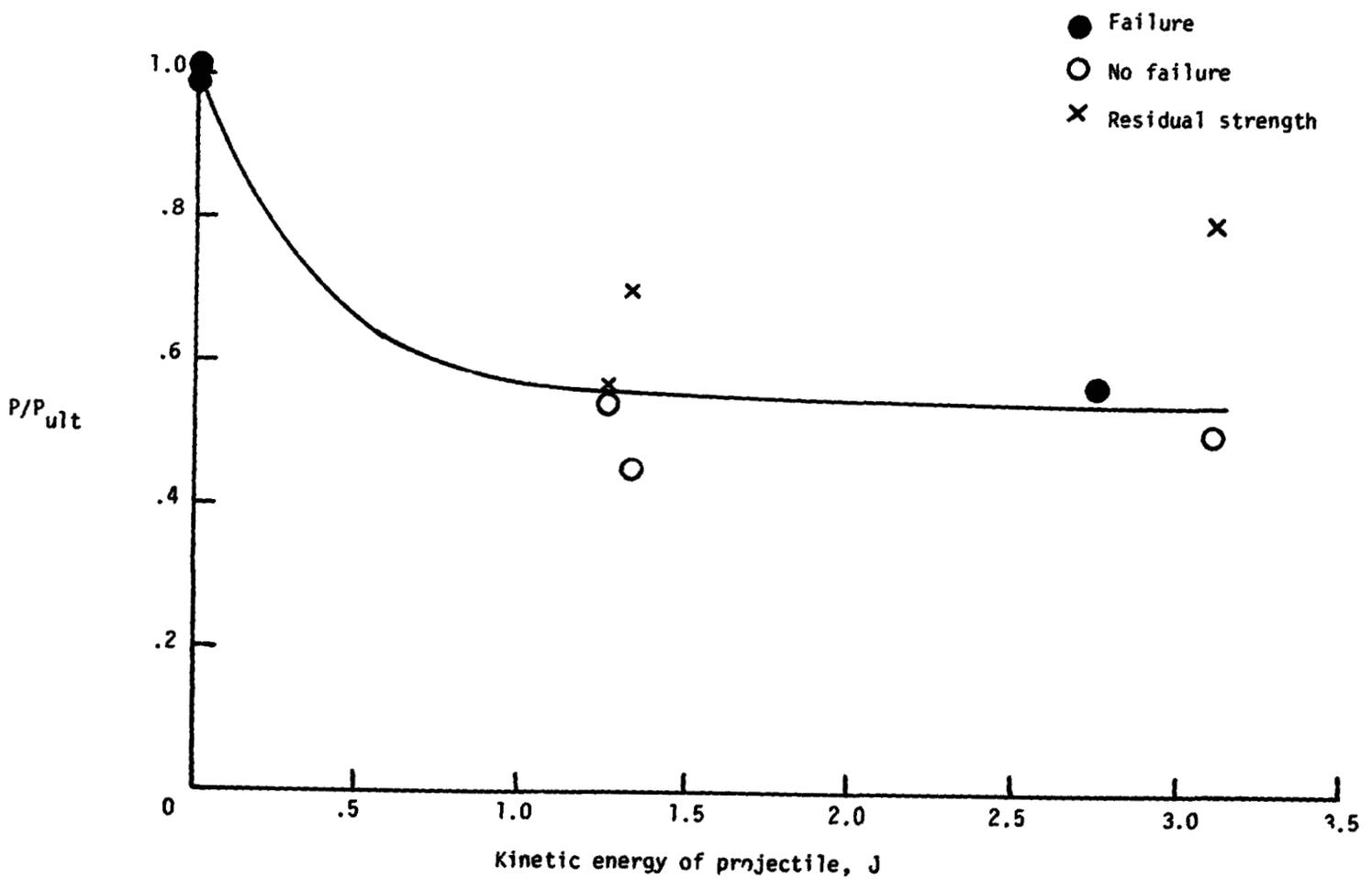

(c) $[90/\pm45/0]_S$ graphite tape.

Figure 11.- Continued.

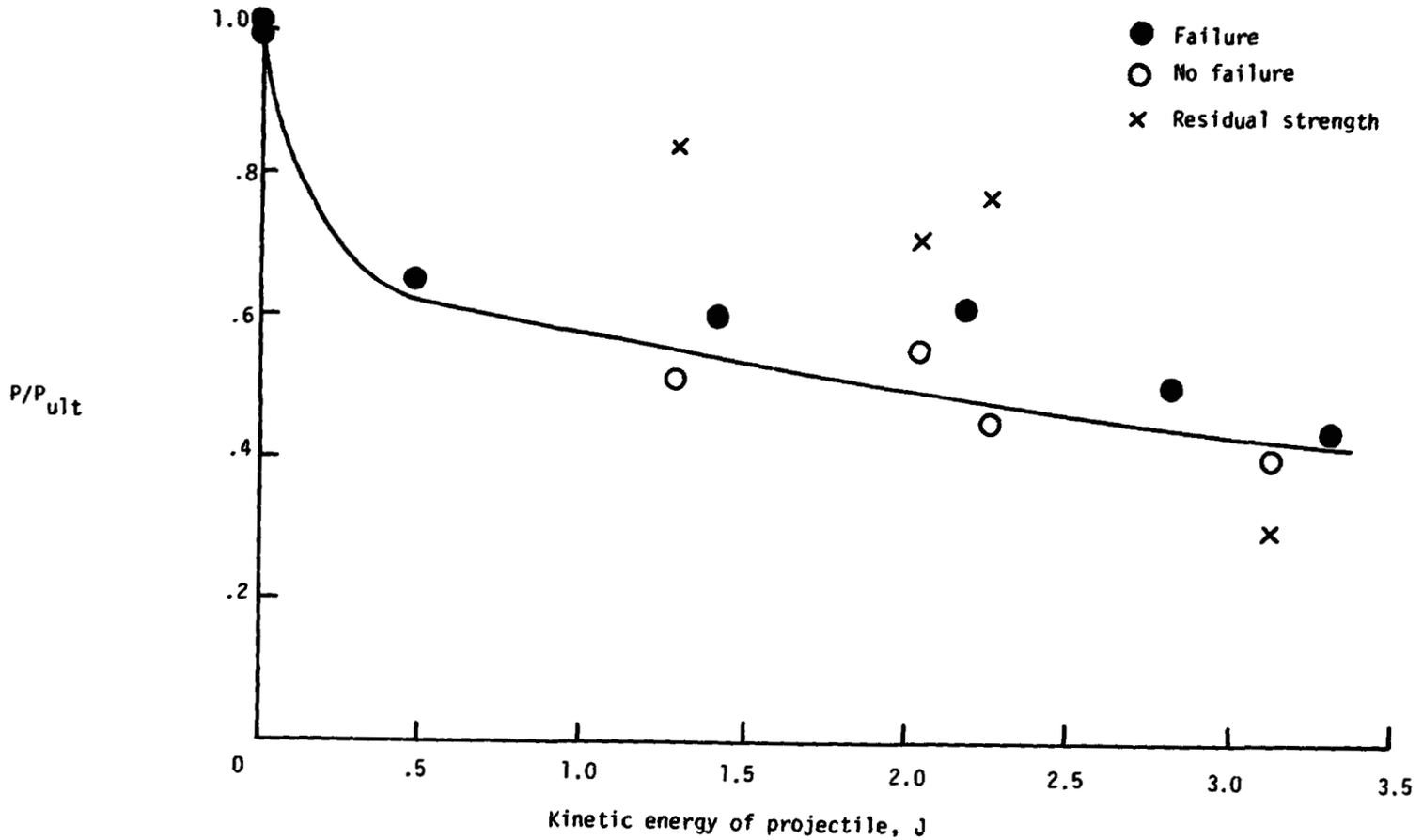

(d) $[45_{GB}/(0_G)_4]$ hybrid of 181-style graphite fabric and graphite tape.

Figure 11.- Continued.

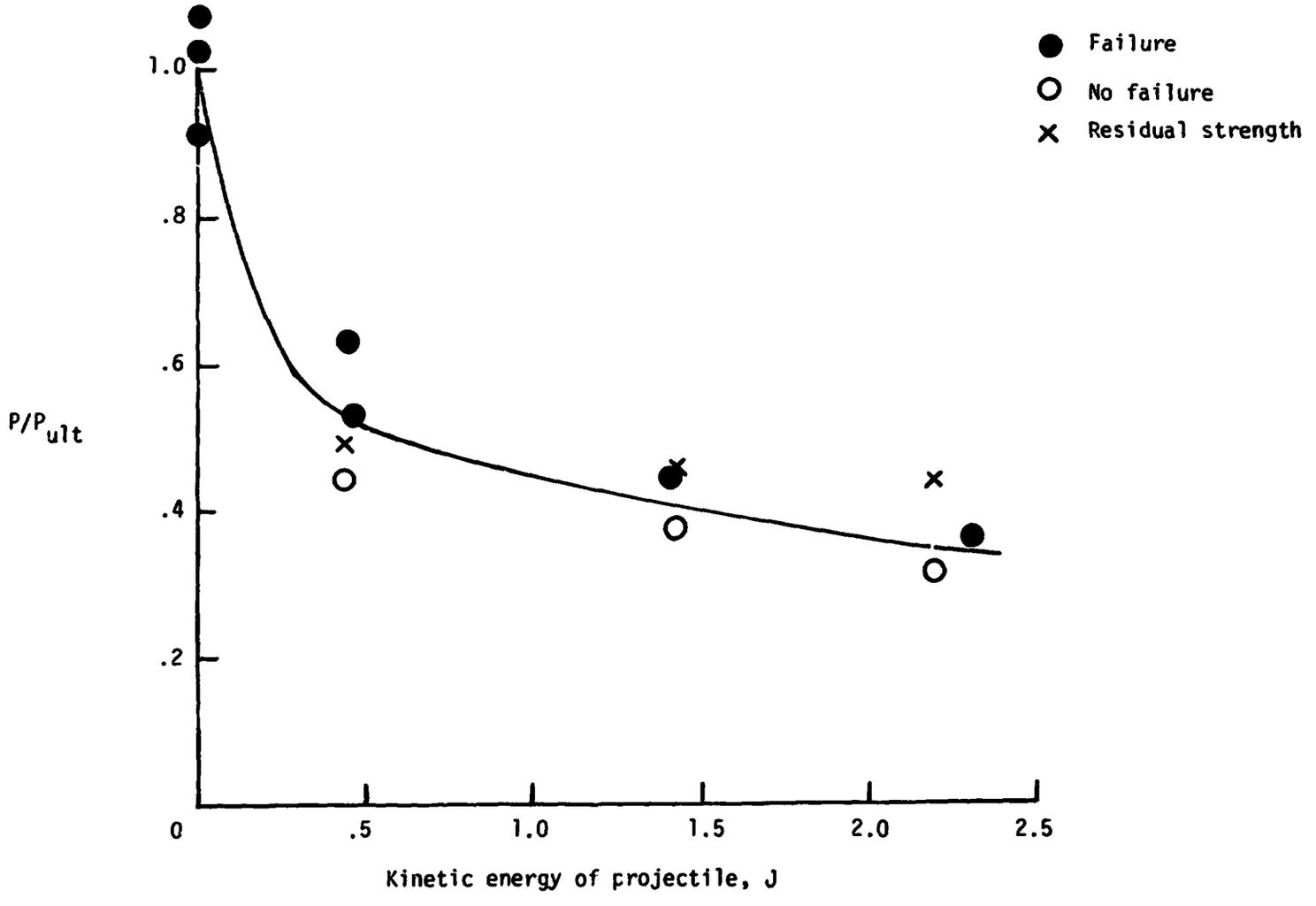

(e) $[45/0/-45/0]_S$ graphite tape.

Figure 11.- Concluded.

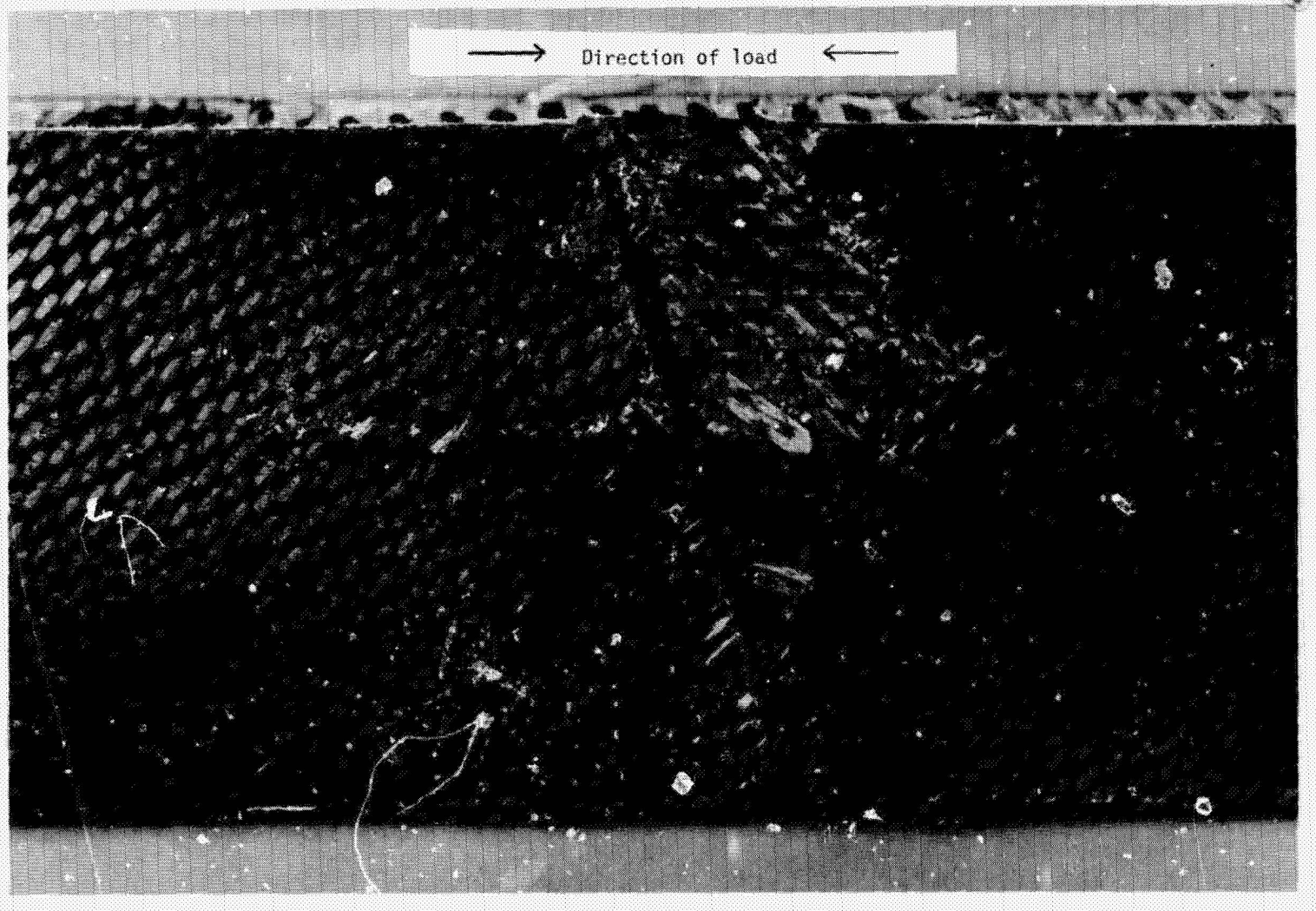

L-78-117

Figure 12.- Failure of a typical $[45_{GB}/(0_G)_4]_S$ graphite/epoxy laminate loaded in compression.

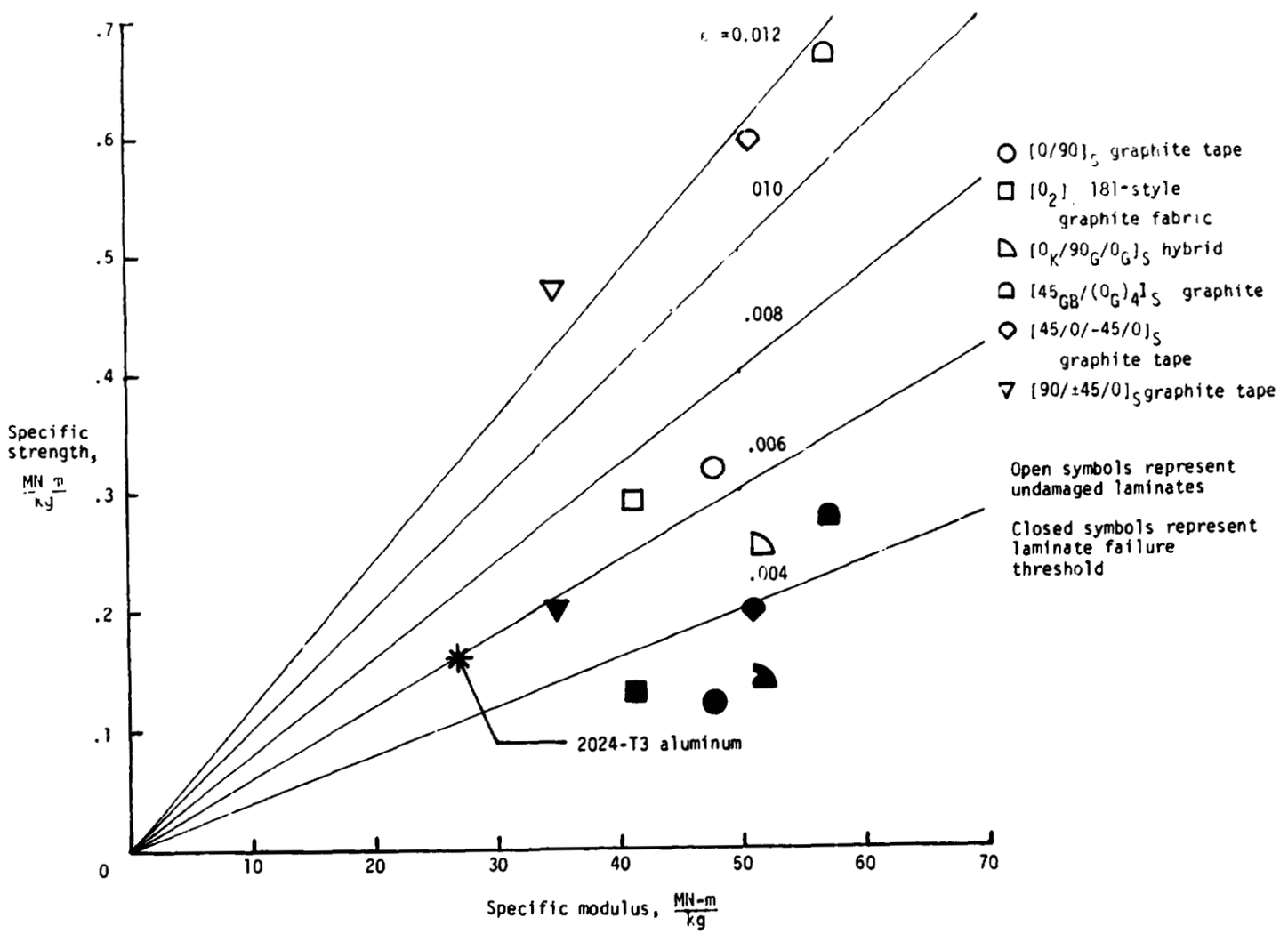

Figure 13.- Specific compression strength as a function of specific compression modulus of test laminates in the unc maged condition and at the failure threshold, compared with a typical aluminum.